https://doi.org/10.5194/egusphere-2026-4552
Preprint. Discussion started: 25 August 2026

Measurement report: Distinct urban and rural organonitrate formation regimes in a mixed anthropogenic-biogenic subtropical atmosphere

Shan Huang[1,2*], Lina Wu[1,2], Yi Kuang[1,2], Yuan Liu[1,2], Weiwei Hu[3], Ye Kuang[1,2], Wei Li[1,2], Qicong Song[1,2], Yuwen Peng[1,2,#], Suxia Yang[1,2,§], Mingfu Cai[1,2,ǂ], Duohong Chen[4], Dingli Yue[4], Wei Song[3], Bin Yuan[1,2], Xinming Wang[3], Min Shao[1,2]

[1]College of Environment and Climate, Jinan University, Guangzhou 511443, China.
[2]Guangdong-Hongkong-Macau Joint Laboratory of Collaborative Innovation for Environmental Quality, Guangzhou 511443, China.
[3]State Key Laboratory of Advanced Environmental Technology, Guangzhou Institute of Geochemistry, Chinese Academy of Sciences, Guangzhou 510640, China
[4]Guangdong Ecological and Environmental Monitoring Center, Key Laboratory of Regional Air Quality Monitoring, Ministry of Ecology and Environment, Guangzhou 510308, China
[#]Now at: Guangzhou Sub-branch of Guangdong Ecological and Environmental Monitoring Center, Guangzhou 510006, China
[§]Now at: Guangzhou Research Institute of Environment Protection Co., Ltd, Guangzhou 510620, China
[ǂ]Now at: Key Laboratory of Ecological Environment Emergency and Sudden Risk Control, South China Institute of Environmental Sciences, MEE, Guangzhou 510655, China

Correspondence to: Shan Huang (shanhuang_eci@jnu.edu.cn)

Abstract. Particulate organonitrates (pON) are important components of secondary organic aerosols and key reservoir of reactive nitrogen, yet their sources and formation pathways in different atmospheric environments remain poorly understood. Here, we present pON measured in field observations at urban and rural sites in Chinese subtropical region utilizing a soot-particle aerosol mass spectrometer (SP-AMS) combined with positive matrix factorization for source- resolved quantification. With comparable fractions of pON (in total nitrates and organics) and similar average concentrations at both sites, contrasting formation regimes for pON were revealed: at the urban site, daytime photochemistry (16%) and regional transport (33%) dominated, whereas nighttime formation was more pronounced (29%) in rural areas. Elevated volatile organic compounds (VOCs) availability may enhance photochemical organonitrate formation, while nighttime formation was favored under NOx-rich conditions, highlighting the distinct sensitivities of the OH- and NO_3-initiated pathways. Evaluation of organonitrate production potentials showed monoterpenes, isoprene, alkanes, and aromatics dominated the OH-initiated pathway, while styrene and phenols were important NO_3-initiated precursors. Despite overall dominance of biogenic VOCs, anthropogenic VOCs contributed remarkably (59%) to rural organonitrate formation. Refractory pON associated with biomass burning and nighttime formation appeared at the rural site, representing a fraction largely missed by conventional AMS. Our results demonstrate a pronounced urban-rural shift in pON formation regimes, where anthropogenic precursors unexpectedly influence nocturnal chemistry at the rural site, highlighting the complexity of organonitrate formation in mixed anthropogenic–biogenic subtropical environments and the need to consider refractory pON in future studies.

https://doi.org/10.5194/egusphere-2026-4552
Preprint. Discussion started: 25 August 2026

1 Introduction

Organonitrate (ON), i.e., esters containing nitrate functionality (-ONO_2), has been identified as a key component impacting secondary organic aerosol (SOA) formation and nitrogen oxides level by acting as a reservoir (Perring et al., 2013), consequently influencing regional air quality (Bertman et al., 1995) and ozone formation (Mao et al., 2013; Perring et al., 2013). Particle-phase organonitrates (pON) can contribute 5% to 77% of OA mass concentration (Ayres et al., 2015; Boyd et al., 2015; Fry et al., 2013; Ng et al., 2017; Rollins et al., 2012; Xu et al., 2015a; Yu et al., 2019), particularly explaining 27-40% of the nighttime SOA growth (Rollins et al., 2012). ON acts as both a sink and a source of reactive nitrogen oxides (Andersen et al., 2025; Farmer et al., 2011), linking key components of atmospheric chemistry including SOA, Volatile Organic Compounds (VOCs), O_3, and NO_X. Moreover, nitration of organics especially aromatic compounds may significantly enhance the toxicity of the products (Albinet et al., 2008; Ning et al., 2020; Yang et al., 2010), making ONs a potential risk to human health (Fernández et al., 1992). Therefore, a better understanding of atmospheric concentrations, formation mechanism and controlling factors for ON is highly needed.

ON can be formed via OH-initiated photooxidation of VOCs in the presence of NO_X and via NO_3-initiated oxidation of VOCs (Liebmann et al., 2019; Ng et al., 2017; Rollins et al., 2012) . Also, O_3 can oxidize VOCs especially alkenes, via Criegee intermediates, to produce OH and RO_2, then leading to alkyl nitrates in the presence of NO (Liebmann et al., 2019). Most previous studies have focused on ON formation under conditions dominated by biogenic precursors (Andersen et al., 2025; Kiendler-Scharr et al., 2016; Lee et al., 2016b; Ng et al., 2017; Walters et al., 2025; Xu et al., 2015a), while the role of anthropogenic VOCs (AVOCs) remains less investigated. Field studies (Lee et al., 2019; Lee et al., 2015) have shown that intermediate-volatile organic compounds (IVOCs) and anthropogenic alkanes can contribute significantly to pON through photo-oxidation. Aromatic precursors such as toluene (Ramasamy et al., 2019) and styrene (Yu et al., 2019) can be oxidized by NO_3 radicals to form pON. In addition, biomass burning (BB) and fossil fuel combustion can directly emit pON (Gaston et al., 2016; Lin et al., 2021; Zhang 2016), while VOCs in BB plumes can undergo secondary reactions to produce pON (Ahern et al., 2019; Joo et al., 2019). These results suggest that the sources, formation pathways and dominant precursors of pON are highly dependent on local emissions characteristics and atmospheric conditions.

Based on existing field studies using aerosol mass spectrometry (AMS), ambient mass concentrations of organic nitrate (corresponding to -ONO_2 functionality) typically ranged from approximately 0.05 to 1 μg m^{-3} though they could vary dramatically from 0.01 to approximately 7 μg m^{-3} (Fry et al., 2013; Ge et al., 2022; Kiendler-Scharr et al., 2016; Ng et al., 2017; Rollins et al., 2012; Xu et al., 2015b; Xu et al., 2021a; Yu et al., 2019; Zhu et al., 2021; Zhu et al., 2016), with substantial regional variability in their sources and formation processes. Previous studies have often reported associations between pON and specific OA factors (e.g., less-oxidized oxygenated OA, LO-OOA or semi-volatile oxygenated OA, SV-OOA), suggesting links to nocturnal NO_3 chemistry and biogenic VOCs in regions such as Europe (Kiendler-Scharr et al., 2016) and southeastern United States (Xu et al., 2015b). Also, Lee et al. (2016a) found that pON contributed 22-33% to biogenic SOA (BSOA) mass during nighttime in a coniferous forest. In contrast, a study in Africa pointed out that pON accounted for a lower percentage

https://doi.org/10.5194/egusphere-2026-4552
Preprint. Discussion started: 25 August 2026

of OA (5%) and was more likely to be derived from long-range transport in Central Africa than local formation (Brito et al., 2018). In China, nighttime secondary formation (LO-OOA) was found to correlate well with ON in the Shenzhen (Yu et al., 2019), a megacity in South China, while in rural North China Plain (Xianghe), ON was more closely associated with BB in summer (Zhu et al., 2021), or secondary formation especially aqueous-phase processes in winter (Huang et al., 2021). Although these findings indicate the dependence of pON sources and formation pathways on regional emission characteristics, more detailed observational constraints that link emissions, VOC precursors, and formation pathways are still limited, particularly across contrasting environments such as urban and rural regions. In addition, while the role of non-refractory pON has been often investigated, the contribution of refractory pON associated with combustion-derived particles and its implications for formation pathways remain poorly understood.

In this study, we investigate the sources and formation pathways of pON based on field measurements at urban and rural sites in the Pearl River Delta (PRD), China, utilizing a Soot Particle-High-resolution time-of-flight aerosol mass spectrometer (referred to as SP-AMS). The pON was quantified using positive matrix factorization (PMF) and evaluated against an independent method. By integrating PMF-resolved sources with VOC precursor information and estimated organonitrate production potential, we provide observational constraints on pON formation pathways. Especially, we examine the contrasting roles of anthropogenic and biogenic precursors under different atmospheric conditions and assess the contribution of refractory pON enabled by the unique capability of SP-AMS to detect particles associated with black carbon (BC) and brown carbon (BrC). The analysis mentioned above provides new insights into the coupling between emission sources, precursor chemistry, and formation processes of pON in urban and rural environments.

2 Methods

2.1 Field measurements

The comprehensive field observations for physical and chemical properties of atmospheric pollutants including gases and particles were performed at an urban site (Guangzhou) and rural site (Heshan) respectively in autumn of 2018 and 2019 (Fig. S1), a season with frequent air pollution in PRD (Hou et al., 2019). The urban site was at the Guangzhou Institute of Geochemistry, Chinese Academy of Sciences (GIG, 23.1°N, 113.2°E), surrounded by residential buildings and two main traffic roads. The rural site was at a supersite in Heshan county (22.7°N, 112.9°E), a downwind receptor 50~80 km southwest of PRD central cities Foshan and Guangzhou, often influenced by urban plumes. Both sites are located in the subtropical region, which is characterized by warm, humid conditions and abundant vegetation cover throughout the year.

During two field observations, an SP-AMS was deployed to measure non-refractory and refractory submicron aerosol components with high time and mass resolution. Particle size distribution (PNSD, 13-650 nm) was measured by a scanning mobility particle sizer (SMPS). VOCs were measured by online gas chromatography-mass spectrometry/flame ionization detector (GC-MS/FID) and proton transfer reaction time-of-flight mass spectrometry (PTR-ToF-MS). Trace gases including

https://doi.org/10.5194/egusphere-2026-4552
Preprint. Discussion started: 25 August 2026

O_3, NO_X, CO and meteorological parameters including wind speed (WS), wind direction (WD), temperature (T), relative humidity (RH) and air pressure were supplied by the local authorities. Several pON species were provided by an iodide-adduct Filter Inlet for Gases and AEROsols - Chemical Ionization Mass Spectrometer (FIGAERO- CIMS) and used for validation (hereafter referred to as CIMS). The details of instruments (e.g. mode, manufactures, time resolution) are listed in Table S1. The analysis in this study focuses on data obtained from two autumn campaigns from 16 Oct. to 20 Nov. 2018 (urban site) and 15 Oct. – 17 Nov. 2019 (rural site).

2.2 SP-AMS operation and Data analysis

SP-AMS measures non-refractory PM_1 species (organics, ammonium, nitrate, sulfate and chloride) and refractory BC (rBC) and associated coatings with an embedded Nd:YAG laser vaporizer (1064 nm, ~4000K) (Onasch et al., 2012). The instrument principle of SP-AMS has been reported previously by (Onasch et al., 2012). At both sites, the SP-AMS was operated switching between V-mode (tungsten vaporizer only) and SP-mode (both laser and tungsten vaporizer). The time resolution for each run was 1 min. At the urban site, routine calibrations were performed, providing ionization efficiency (IE) and speciated relative ionization efficiency (RIE) used in this study (sulfate: 1.5, nitrate: 1.1, chloride: 1.3, organics: 1.4, and ammonium: 4.7). At the rural site, due to calibration issues, default RIEs are applied (sulfate: 1.2, nitrate: 1.1, for chloride: 1.3, organics: 1.4 and ammonium: 4.0), and data quality was assured by good agreement with external measurements and presented in our previous study (Kuang et al., 2021). The composition dependent collection efficiency (CDCE) (Middlebrook et al., 2012) were used at both sites. Data were processed using the Igor-based AMS data analysis software SQUIRREL (v1.21E), for unit mass resolution (UMR) data and PIKA (v1.61E) for high resolution (HR) data. The toolkit HistBox (Wu et al., 2018) was also used for further data analysis. PM_1 component mass concentrations derived from HR data were averaged to 10min (urban) and 15min (rural).

For source apportionment of organic aerosols (OA), PMF analysis (Paatero, 1997; Paatero and Tapper, 1994) was performed separately on the urban and rural OA datasets using the PET v3.05 (Ulbrich et al. 2009). PMF input data includes organic ion mass concentrations and uncertainty matrices from SP-AMS HR data. Isotopes and ions with m/z >120 were excluded before PMF running. For both sites, a six-factor solution was chosen for pure OA PMF (PMF_{org}) based on diagnostic of parameters and physical meaning identification (Table 1), detailed in our previous studies (Kuang et al., 2021; Kuang et al., 2025; Liu et al., 2023; Wu et al., 2024a), which was the basis of ON quantification in the following analysis.

https://doi.org/10.5194/egusphere-2026-4552
Preprint. Discussion started: 25 August 2026

Table 1. OA factors identified at the urban and rural sites.

Urban		Rural	
OA Factor	**Full name and identified source**	**OA Factor**	**Full name and identified source**
	Primary OA		
HOA	Hydrocarbon-like OA; primary traffic/fossil fuel combustion emissions	HOA	Hydrocarbon-like OA; primary traffic/fossil fuel combustion emissions
COA	Cooking-related OA; local primary cooking emissions	BBOA	Biomass burning OA; primary biomass burning emissions
NOA	Nitrogen-containing OA; primary emissions with amine		
	Secondary OA		
LOOA	Less-oxygenated OA; daytime photochemical oxidation	LOOA	Less-oxygenated OA; daytime photochemical oxidation
MOOA	More-oxygenated OA; mainly from regional transport	MOOA	More-oxygenated OA; mainly from regional transport
aBBOA	Aged biomass burning OA; aged components of biomass burning emissions	Night-OA	Nighttime-formed OA; nocturnal SOA formation related
		BBSOA	Biomass burning-related SOA; SOA formation from biomass burning emitted precursors

2.3 Quantification of organic nitrates

2.3.1 Particulate ON quantification by PMF methods

Based on SP-AMS data, two approaches were applied to quantify ON including PMF method and NO^+/NO_2^+ (referred to as NO_X ratio) method. Briefly, PMF method is integrating NO^+ and NO_2^+ ions obtained from HR AMS data into pure organic spectral matrix for PMF analysis ($PMF_{Org+NOx}$), which usually can separate inorganic nitrate and organic nitrates in different OA factors. Also, facilitated by laser on mode of SP-AMS, both non-refractory components and refractory components (usually BC and BC-coatings) are detected, which were combined in PMF to characterize pON in refractory components. We ran PMF ($PMF_{Org+Cx+NOx}$) with data from laser on mode, including HR organic ions, C_x^+(C_1^+~C_9^+) ions, NO^+ and NO_2^+ ions, and obtained different factors with identified sources. Factors from $PMF_{Org+NOx}$ and $PMF_{Org+Cx+NOx}$ were identified by well correlations with corresponding factors in PMF_{Org} or $PMF_{Org+NOx}$ (Tables S2 and S3), also linking to different sources and processes. Details of abovementioned PMF solution validation at two sites are provided in Text S1. In both urban and rural campaigns, one inorganic nitrate factor (Inorg-NO_3) and 6 $PMF_{Org+NOx}$ factors are recognized with the same name as PMF_{Org} (Table 1). Nitrate function group (-ONO_2) for organonitrates (referred to as $NO_{3,org}$, same as below) from different sources can be calculated as a sum of NO^+ and NO_2^+ extracted from factor mass spectra and mass concentrations (Xu et al.,2015b), and then pON mass concentration can be estimated using an average of 250 g mol^{-1} for the molecular weight of organonitrates (Rollins et al., 2012).

https://doi.org/10.5194/egusphere-2026-4552
Preprint. Discussion started: 25 August 2026

The other method, NO_X ratio method, distinguishes organic nitrates (ON) from inorganic nitrate using their distinct NO^+/NO_2^+ ratio (Boyd et al., 2015; Bruns et al., 2010; Day et al., 2022; Farmer et al., 2010) and have been widely used for ON quantification. In this study, we use ON values (upper- and lower-bound) estimated by NOx ratio method as a reference based on the multiple inter-comparisons (Section 3.1). More details of calculation using this method can be found in Text S2.

2.3.2 Estimation of ON production potential (PPON)

Organic nitrates can be formed by oxidation of VOCs via OH-initiated, NO_3-initiated and O_3-initiated pathways. To assess the formation potential from each pathway, theoretical production potential of gas-phase organonitrates (PP_{ON}) could be calculated with following equations (Liebmann et al., 2019):

$$PP_{OH} = \alpha_i^{RO2} \times k_{OH+VOC_i} \times [VOC]_i \times [OH] \quad (1)$$

$$PP_{NO_3} = \alpha_i^{NO3} \times k_{NO_3+VOC_i} \times [VOC]_i \times [NO_3] \quad (2)$$

$$PP_{O_3} = \alpha_i^{O3} \times \alpha_i^{RO2} \times k_{NO_3+VOC_i} \times [VOC]_i \times [OH] \quad (3)$$

where PP_{OH}, PP_{NO_3}, and PP_{O_3} are estimated PP_{ON} via OH-initiated, NO_3-initiated and O_3-initiated pathways, respectively. α_i^{RO2} is the ON formation branching ratio for the oxidation of a specific VOC_i initiated by OH radical (forming peroxy radicals, which then react with NO). α_i^{NO3} and α_i^{O3} present the yields of ON from the reaction of VOC_i with NO_3 radical and from the O_3-initiated reaction (forming peroxy radicals), respectively. $[VOC]_i$ is the concentration of specific VOC_i (ppbv). k is the corresponding reaction rate coefficient (molecules cm^3 s^{-1}), and [OH] and [NO_3] represent the concentrations of OH and NO_3 radicals, obtained from Master Chemical Mechanism (MCM) box model simulation (Yang et al., 2022). In this study, the fraction of RO_2 radical going to reaction with NO (rather than HO_2) was assumed to be 1, which has been validated in our previous study (Cai et al., 2023). For the O3-initiated pathway, only isoprene and monoterpenes were considered due to the availability of reported ON yield parameters. All parameters used for PPON calculation are listed in Table S4.

Based on current knowledge, only a few VOCs (e.g., monoterpenes, isoprene) have organic nitrate yields (α) for the NO_3 and O_3 oxidation pathway (Table S4). Therefore, a unity yield (α = 1) was assumed for the rest VOCs with NO_3-initiated pathway in this study, which does not change the dominating roles of monoterpenes and isoprene (detailed in Section 3.5). Meanwhile, since monoterpenes could not be separated from the $C_{10}H_{17}$ alkene measured by PTR-ToF-MS, we assume that the contributions of limonene and α-pinene are 1:1 in the PPON calculation.

3 Results and discussion

3.1 Intercomparisons and evaluation of pON

To evaluate the reliability of pON quantification, multiple approaches were compared, including the PMF-based method, the NOx ratio method, and an independent CIMS measurement. Figure 1 showed comparisons of organonitrate derived from different methods. Strong correlations were found between $NO_{3,org}$ estimated by the AMS-PMF and pON measured by CIMS

https://doi.org/10.5194/egusphere-2026-4552
Preprint. Discussion started: 25 August 2026

at both sites (R=0.65~0.68). Whereas, the NOx ratio method showed much weaker agreement (R = 0.02~0.21) with CIMS results, as well as with PMF method (R= 0.28~0.35) as shown in Fig. S10, lower than those reported in Shenzhen (R=0.77-0.82) (Yu et al., 2019) and Xianghe (R=0.76) (Zhu et al., 2021). Also, larger discrepancies between the AMS-PMF method and CIMS were generally found under conditions of high total nitrate mass concentrations (>10 μg m^{-3}, Fig. 1a, c). A possible reason is that at high concentrations, nitrate was predominantly inorganic, leading to greater uncertainty in separating organic nitrate from total nitrate.

At the urban site, average $NO_{3,org}$ concentration and its fraction in total nitrate from PMF method broadly fall within the range derived from NOx ratio method (Fig. 1b), that is, 0.56±0.45 μg m^{-3} and 18%, while at rural site, both (0.65±0.24 μg m^{-3} and 16%) were close to the lower bounds estimated by the NOx ratio method (Fig. 1d). The fractions of $NO_{3,org}$ in total nitrate from both methods were also similar at the two sites (18% and 16%, respectively), comparable with previous studies (Yu et al., 2019; Zhu et al., 2021). Although CIMS captured only a fraction of total organonitrate, its stronger correlation with PMF-derived $NO_{3,org}$ than NOx ratio method supports the reliability of the PMF-method in the case of this study. Therefore, the PMF method was adopted in the following analysis to represent pON. Also, $NO_{3,org}$ represents only the mass concentration of nitrate functional groups. When converted to total organonitrate mass by accounting for molecular weight, the resulting pON estimated from AMS-PMF would be substantially increased.

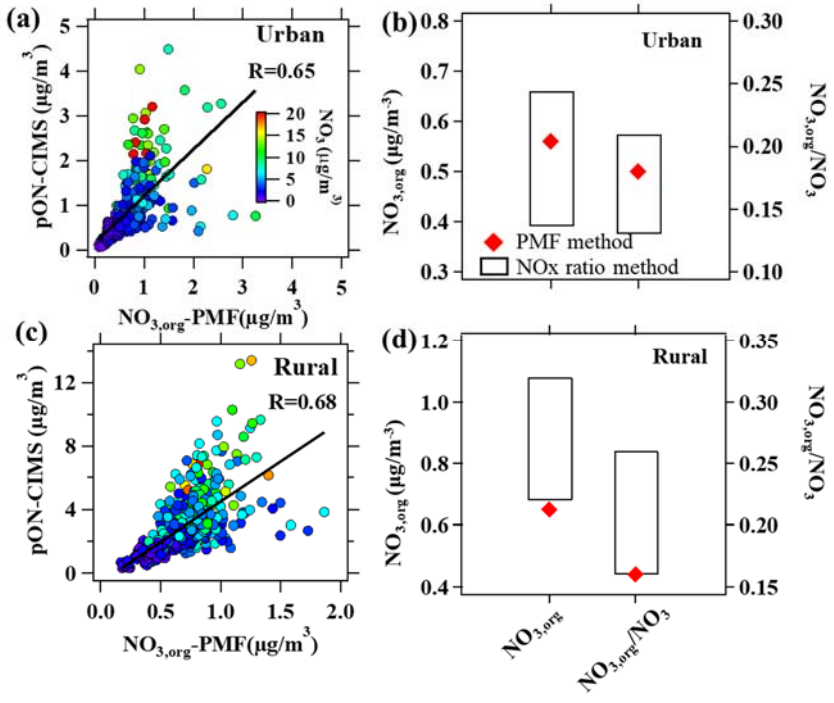

Figure 1: Comparison between pON mass concentrations from CIMS and $NO_{3,org}$ from AMS-PMF method at (a) urban and (c) rural sites. Average mass concentrations and fractional contributions to total nitrate of $NO_{3,org}$ from AMS-PMF and AMS-NOx ratio methods are shown at (b) urban and (d) rural sites. The upper and lower edges of boxes represent the upper and lower bounds estimated by NOx ratio method.

https://doi.org/10.5194/egusphere-2026-4552
Preprint. Discussion started: 25 August 2026

3.2 Mass concentrations of pON at both sites

An overview on organonitrates quantified by PMF method, together with major aerosol components, gaseous pollutants and meteorological parameters during two campaigns was provided in Fig. 2. In general, during the urban measurement, winds were predominantly from the northeast with relatively high speed (4.29±2.30 m s^{-1}, up to 13.2 m s^{-1}), while winds at the rural site were mainly from the southwest with lower speed (1.54±0.73m s^{-1}). Gaseous NO_X (NO and NO_2) mainly associated with vehicle emissions, was approximately twice at the urban site as at the rural site. However, the average PM_1 mass concentration was lower during the urban campaign (29.93±19.95 μg m^{-3}) than during the rural campaign (40.02±15.48 μg m^{-3}).

Submicron particles presented similar chemical composition at both sites, dominated by the organics (57% and 52% at urban and rural sites, respectively), followed by sulfate (15% and 17%), nitrate (10% at both sites), BC (8% and 10%), ammonium (7% and 9%), and chloride (2% at both sites). $NO_{3,org}$ concentrations at both sites spanned over two orders of magnitude (0.03~6.43 μg m^{-3}), and $NO_{3,org}$ average concentration was higher at the rural site (0.65±0.24 μg m^{-3}) than that at the urban site (0.56±0.45 μg m^{-3}). These average values are within the range of organic nitrates average concentrations reported in previous measurements, such as 0.03~1.32 μg m^{-3} in US and Europe (Ng et al., 2017 and references therein), and 0.07~2.5 μg m^{-3} in China (Ge et al., 2022; Xu et al., 2021a; Yu et al., 2019; Zhu et al., 2025), but higher than those in the other PRD city (0.07~0.39 μg m^{-3})(Yu et al., 2019). The average contributions of $NO_{3,org}$ to the total nitrate (16~18%) are within the range of 10~33% reported in the previous autumn studies using PMF method (Ge et al., 2022 and references therein). Its contribution decreased with increasing nitrate mass concentration at both sites (Fig. 2b,c), agreeing with the observations at worldwide sites (Day et al., 2022; Huang et al., 2021) as well as our other study in PRD (Liao et al., 2026). This variation indicates that increasing inorganic nitrate under polluted conditions may suppress the contribution of pON, and meanwhile, highlights the significance of organic nitrates in particulate nitrate under relatively clean conditions. Converting with molecular weight, pON was estimated to contribute 13% to total OA on average at both sites, respectively, consistent with other study in PRD (9~20%) (Yu et al., 2019), and reasonably lower than the contribution of N-containing organic molecules to ambient OA (37~50%) (Yu et al., 2024).

Similar $NO_{3,org}$ loadings were found between day and night at the urban site, while more organonitrate was observed during nighttime (0.68±0.26 μg m^{-3}) than daytime (0.60±0.23 μg m^{-3}) at the rural site (Fig. 2d). This contrast suggests a stronger influence of nocturnal formation and accumulation in the rural environment, while pON at the urban site was affected by both daytime and nighttime processes. Furthermore, $NO_{3,org}$ at the rural site was characterized by a pronounced early-evening peak around 18:00 and a slight elevation at midnight, which remained after normalization to boundary layer height (Fig. S11), suggesting a sustained nocturnal source of organic nitrates. The urban site, by comparison, displayed little day-night difference, underscoring the distinct temporal behaviors of organonitrate at the rural and urban sites of PRD.

https://doi.org/10.5194/egusphere-2026-4552
Preprint. Discussion started: 25 August 2026

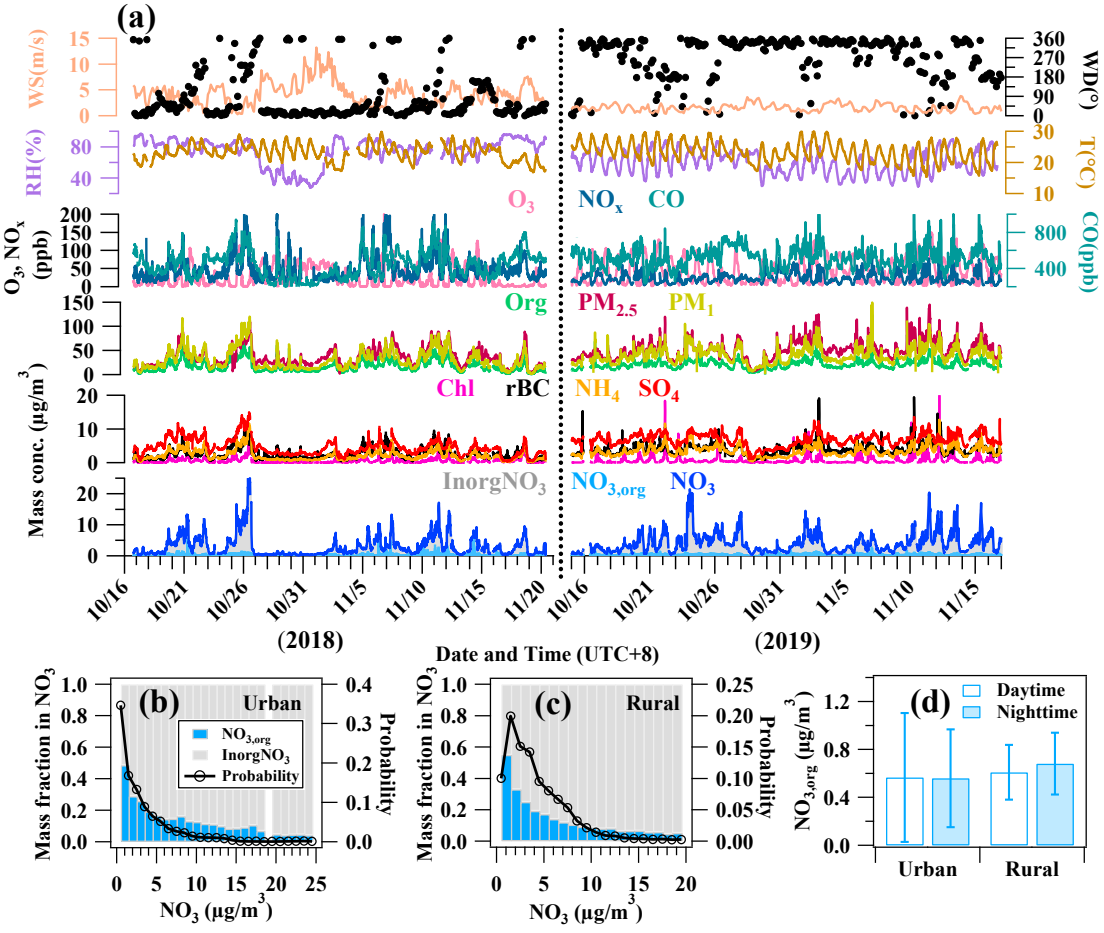

Figure 2: (a) Time series of measured parameters and $NO_{3,org}$ resolved by the AMS-PMF method in the urban (left panel) and rural (right panel) campaigns. Fraction of $NO_{3,org}$ and inorganic nitrate in total nitrate as a function of total nitrate mass concentration (binned to mass concentration intervals of 1 μg m^{-3}) at (b) urban and (c) rural sites. (d) Daytime and nighttime averaged $NO_{3,org}$ concentrations. Error bars represent the standard deviations of the mean concentration. Local time (UTC+8) is used here and in all following figures.

3.3 Formation pathways and source contribution of pON

3.3.1 Biomass burning influence

Facilitated by the PMF method, source and processes of pON were identified and are shown in Fig. 3 using the same factor nomenclature described in Table 1. At both sites in the PRD, BB-related sources were the important contributors to pON, accounting for 25% and 34% of total ON at the urban and rural sites, respectively. Open burning biomass is forbidden in the urban area, so no fresh BB emissions were identified at the urban site, and BB-related pON was mainly associated with aged products (aBBOA). These aged components might originate from domestic or agricultural biomass/biofuel burning during nighttime in the vicinity of Guangzhou (Ye et al., 2021; Yuan et al., 2010), similar to observations reported in other megacities

https://doi.org/10.5194/egusphere-2026-4552
Preprint. Discussion started: 25 August 2026

such as Delhi (Lalchandani et al., 2021) and Beijing (Duan et al., 2004). In contrast, prevailing nighttime BB events, usually around 18:00, were observed at the rural site, where both fresh emissions (BBOA) and secondary products (BBSOA) were found and contributed to ambient organonitrates.

The mass spectra profiles of BB-related OA were characterized by prominent m/z 60 (mainly $C_2H_4O_2^+$) and m/z 73 (mainly $C_3H_5O_2^+$), which are commonly used as BB tracers in the ambient studies(Lanz et al., 2007). In this study, relatively high fraction of m/z 60 (f60) for BBOA at rural site (0.52%) and for aBBOA (0.47%) at urban site fall within the range reported for open straw burning (f_{60}=0.3%-0.6%) (Fang et al., 2017). Increasing NO_X observed at both sites during the early evening (Fig. S12) might also be influenced by BB events, which can then supply NO_3 radicals for nighttime ON formation. Further evidence is provided by the diurnal coincidence between BB-related $NO_{3,org}$ and nitrocatechol ($C_6H_5NO_4^+$), a BB oxidation product (Bertrand et al., 2018)(Fig. S12), suggesting continued evolution of BB plumes involving reactive nitrogen (Ahern et al., 2019; Joo et al., 2019).

At the rural site, an early-evening peak of $NO_{3,org}$ associated with BBSOA was observed approximately one hour after the peak of fresh BBOA (Fig. 3d), consistent with rapid oxidation of BB -related precursors followed by gas-to-particle partitioning (Kuang et al., 2021; Kuang et al., 2025). The noon-peak of $NO_{3,org}$-BBSOA, lower than the early-evening peak but still pronounced, was related to the BBOA concentration during the preceding night (R=0.51,(Wu et al., 2024a)), indicating continued daytime photo-oxidation of residual BB emissions. This interpretation is further supported by the co-increase of $NO_{3,org}$-BBSOA with air temperature (Fig. S14b), as temperature may reflect solar radiation, which can enhance photochemical transformation of ON. In addition, ON associated with BBSOA also slightly increased with elevating RH (Fig. S14a), which might be related to continuous accumulation during the night, suggesting high RH may promote gas-to-particle partitioning of gas phase organonitrate, since increased RH may enlarge aerosol surface area for the uptake of high functionalized ON (George et al., 2015; George and Abbatt, 2010). Nevertheless, $NO_{3,org}$-aBBOA at the urban site showed no correlation with either RH or air temperature (Fig. S13), indicating the different pathway from that from BBSOA at the rural site.

Although the observed O:C and N:C of BBOA (O:C=0.50, N:C=0.052) were slightly higher than those of BBSOA (O:C =0.44, N:C=0.047), BBSOA contributed more to total pON than the fresh BBOA at the rural site (22% vs 12%). This difference may reflect distinct formation pathways. Organonitrates associated with BBSOA were likely formed through rapid oxidation of BB-emitted VOC precursors in presence of reactive nitrogen such as NOx or NO_3 radical (Kuang et al., 2025), while $NO_{3,org}$ associated with BBOA was released from direct combustion of nitrogen-contained biomass (Kuang et al., 2021). Although biomass burning influence on pON has been suggested in previous studies in China, it was often embedded in broader SOA factors (Yu et al., 2019; Zhu et al., 2025). In this study, multiple BB-related factors were separately identified, allowing a more explicit evaluation of BB influences, which may even extend to Night-OA that plausibly involved nighttime oxidation of BB-derived precursors (Section 3.3.3) and was further supported by the refractory ON measurement (Section 3.6). Their substantial contributions, especially at the rural site, highlight the importance of both fresh BB emissions and subsequent processing of BB-derived precursors for pON in rural PRD.

https://doi.org/10.5194/egusphere-2026-4552
Preprint. Discussion started: 25 August 2026

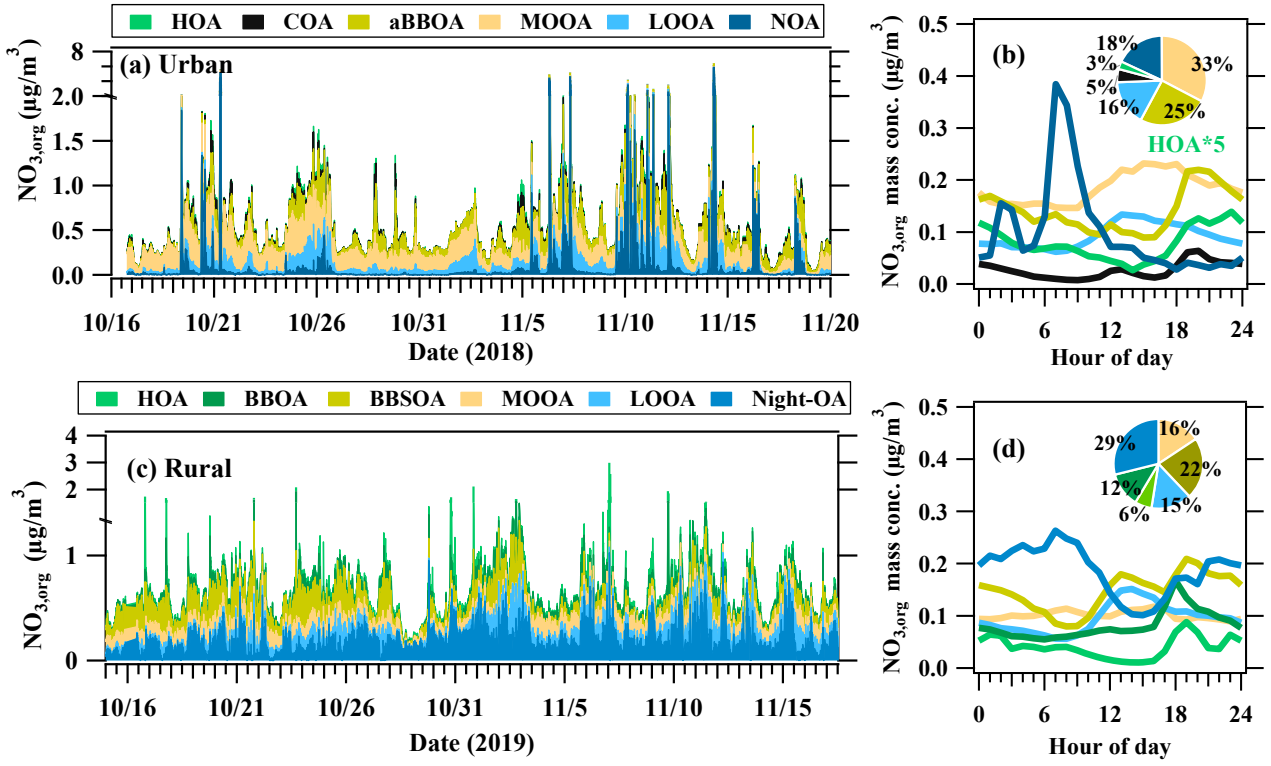

Figure 3: Time series of $NO_{3,org}$ mass concentrations associated with different sources at the (a) urban and (c) rural site. Diurnal variation of $NO_{3,org}$ from different sources at (b) urban and (d) rural sites with their average contributions (pie charts).

3.3.2 Daytime photochemical oxidation

Secondary oxidation was another important pathway of pON formation, and both daytime and nighttime secondary organonitrate formation were identified in this study. At urban and rural sites, $NO_{3,org}$ associate with LOOA was highly correlated to O_x (NO_2+O_3) with R=0.62~0.63. Also, a pronounced noon peak was observed for this factor (Fig. 3b, d), similar as O_3 and Ox (12:00-14:00, Fig. S12). Moreover, its co-increase with temperature (Figs S13, S14) may reflect that LOOA was enhanced by photochemical activity and increased precursor emissions. These features indicate that photochemical oxidation of VOCs by OH radicals in the presence of NO_2 substantially contributed to daytime ON formation.

On average, contribution of photochemically formed organonitrates was similar at urban (16%) and rural (15%) sites, close to the fraction of organic nitrogen associated with less oxidized oxygenated OA (LO-OOA) in Beijing during autumn (17%) (Xu et al., 2017). However, during noontime, the contribution of $NO_{3,org}$ associated with LOOA to total organonitrate increased to about 23% at both sites, implying a significant role of daytime chemistry in pON formation. Furthermore, multiple VOCs, especially BVOCs have been recognized as precursors of daytime ON formation via the OH-initiated pathway (Andersen et al., 2025; Ng et al., 2017; Pullinen et al., 2020; Walters et al., 2025). Based on the measured VOC concentrations, the predominant precursors at both PRD sites are identified by estimating their ON production potentials (see details in the Section

https://doi.org/10.5194/egusphere-2026-4552
Preprint. Discussion started: 25 August 2026

3.5).

3.3.3 Nighttime chemistry

In particular, nocturnal secondary formation represented a major pON source in the rural PRD. $NO_{3,org}$-Night-OA accounted for 29% of total pON and showed elevated mass loadings from evening to early morning (Fig. 3d). Night-OA was strongly correlated with NO_X (R=0.79), suggesting the significance of NO_3-initiated chemistry in nighttime pON formation as found in PRD and other places in the world (Kenagy et al., 2020; Xu et al., 2015a; Xu et al., 2015b; Yu et al., 2019). Compared to other factors, the Night-OA mass spectrum showed a pronounced $C_7H_7^+$ signal at m/z=91.055 ($f_{C_7H_7^+}$=0.97%). This ion has previously been observed in biogenic SOA (BSOA) and has been proposed as a maker for products form monoterpene+NO_3 reactions (Lee et al., 2016a; Nah et al., 2016; Zhou et al., 2019), suggesting that BVOC oxidation may contribute to night formation of pON. However, Night-OA also increased following periods of intense biomass burning, and a similar elevated m/z 91 signal was observed in the BBSOA mass spectrum ($f_{C_7H_7^+}$=0.63%), where $C_7H_7^+$ may also represent aromatics hydrocarbon (McLafferty and Turecek, 1993) emitted from biomass burning. These findings indicate that Night-OA may also be influenced by transformation of BB emissions, possibly representing an important formation pathway of Night-OA-related pON. In addition, our previous study (Kuang et al., 2025) presented that Night-OA had the second strongest light absorptivity after BBOA, and proposed that its formation may involve both gas-phase reactions of BB precursors and aqueous-phase chemistry which accelerates the formation. Consistent with this interpretation, $NO_{3,org}$-Night-OA was positively correlated with RH (Fig. S14a), indicating that aqueous-phase processes may further promote organonitrate growth. The adverse effect of air temperature on nighttime ON formation (Fig. S14b) implies that nocturnal pON was probably semi-volatile, favoring partitioning into the gas phase at higher temperature. This behavior is consistent with previous findings that BVOC oxidation products under high-NO_X conditions were mostly semi-volatile and contributed significantly to the SOA (Xu et al., 2021b).
At the urban site, no specific nighttime formation factor was identified although aBBOA showed a pronounced increase from 18:00 to 21:00. If taking consideration of co-increase of primary emissions (HOA and COA) and offset by BLH for total $NO_{3,org}$ (Fig. S11b), this elevation might be explained by to aging of primary BB emissions together with boundary layer compression.

3.3.4 Aging and transport

Considering that lifetime of particulate organonitrates can reach several hours (Lee et al., 2016b), they may undergo fast regional transport. MOOA, a factor linked to regional transport with continuous aging, was identified at both sites. $NO_{3,org}$-MOOA contributed 16% of total pON at the rural site and 33% at the urban site, indicating a significant contributor for ambient organonitrates. At the rural site, the negligible diurnal variation of $NO_{3,org}$-MOOA indicates that these organonitrates were relatively aged and may partly reflect the regional background level of pON. At the urban site, different diurnal pattern was observed for this factor. $NO_{3,org}$-MOOA gradually increased during the day, beginning around 10:00 and reaching a maximum

https://doi.org/10.5194/egusphere-2026-4552
Preprint. Discussion started: 25 August 2026

near 15:00. This increase, together with the corresponding decrease in $NO_{3,org}$-LOOA (Fig. 3b), suggests a combined effect of further oxidation of LOOA similar as previous study (Sun et al., 2011) and accumulation through regional transport. Moreover, $NO_{3,org}$-MOOA exhibited positive correlation with air temperature (Fig. S13b), which may support this factor was contributed by photochemical oxidation during daytime.

3.3.5 Minor primary sources

Other primary emissions including HOA, COA and NOA contributed only a small fraction of total pON (<26%). Low contribution of HOA-related organonitrate (3% and 6% at the urban and rural sites, respectively) indicates that vehicle exhaust was not a major direct source of pON, consistence with previous studies showing negligible ON in vehicle emissions (Le Breton et al., 2019; Peng et al., 2022). Although HOA showed clear rush hour peaks, $NO_{3,org}$-HOA at the rural site exhibited a stronger nighttime enhancement than at the urban site, probably reflecting the unresolved cooking-related influence from nearby villages (Kuang et al., 2021). At the urban site, cooking emissions were recognized as a specific source (COA) but only contributed 5% of total pON mass, despite reaching 9% during dinner hours (19:00-21:00). Nitrogen-containing compounds emitted from cooking oil have been reported in laboratory studies (Liu et al., 2017), and enhanced organic nitrogen during mealtimes has also been observed in ambient measurements in Beijing (Xu et al., 2017), implying ON can be generated form cooking emissions.

A nitrogen-containing OA (NOA), characterized by prominent amine-related ions (e.g. CH_4N^+ and $C_3H_6N^+$), was identified only at the urban site. Similar to previous studies (Hayes et al., 2013; Sun et al., 2011; Zhang et al., 2013), NOA contributed only 3% to total OA on average, but accounted for a substantially larger fraction of total pON (18%), indicating a disproportionate enrichment of ON in this factor. During periods of elevated NOA abundance (~4.3% of whole campaign), $NO_{3,org}$-NOA reached 1.42 μg m^{-3}, accounting for as much as 72% of total pON. In the city, gaseous amines could be emitted from industry (Hayes et al., 2013; Sun et al., 2011) and sewer pipes (Chang et al., 2021), while the former is not the case in urban Guangzhou. ON in this factor may partly originate from multistep ozonolysis of amines (Ditto et al., 2020; Qiu and Zhang, 2013; Zahardis J, 2008). However, the distinct nighttime (~02:00) and morning (~07:00) peaks (Fig. 3b) suggest that primary emissions were likely the dominant source of this factor.

Taken together, secondary formation dominated pON at both sites (74~82%), consistent with findings in other Chinese megacities, although the dominant pathways differed among atmospheric environments. For example, pON in Shenzhen was strongly associated with LO-OOA, particularly during nighttime (Yu et al., 2019), whereas a distinct Night-OA factor was not resolved in Shanghai (Zhu et al., 2025). In the PRD, daytime photochemical processes contributed 15~49% of pON and were more important at the urban site, while nocturnal formation contributed significantly at the rural site (29%), indicating a greater role of NO_3 -initiated chemistry under rural conditions, similar with previous findings (Kenagy et al., 2020) . Together with substantial BB influence and regional transport, these results highlight considerable variability in the processes controlling pON across different atmospheric environments.

https://doi.org/10.5194/egusphere-2026-4552
Preprint. Discussion started: 25 August 2026

3.4 Influence of VOCs/NOx ratio on pON formation

The VOCs/NOx ratio has been widely used to diagnose the relative roles of VOCs and NOx availability in atmospheric oxidation processes(An et al., 2024; Ren et al., 2022; Sato et al., 2022). Here, we evaluated the relationships between source-resolved organonitrate and the VOCs/NOx ratio at both urban and rural sites (Fig. 4), highlighting differences in the contributions of individual factors to ON formation. At the urban site, $NO_{3,org}$ associated with LOOA and MOOA exhibited a clear positive correlation with the VOCs/NOx ratio (R=0.91~0.96, Slope= 0.09 ~0.15) accompanied by concurrent O_3 enhancement (Fig. 4a), indicating that daytime photochemistry significantly promotes ON formation. The urban VOCs/NOx ratio was relatively low (0.25~2.5), likely reflecting NOx-rich, VOC-limited conditions, and no turning point was observed within this range. This suggests that LOOA- and MOOA-related ON production in the city was promoted by photochemistry under sufficient NOx availability, consistent with previous studies (Ng et al., 2017; Walters et al., 2025). At the rural site, where the VOCs/NOx ratio varied in a broader range (0.75~8), LOOA-related ON exhibited a similar co-increase with VOCs/NOx up to ~5, after which it began to decline (Fig. 4b). Nevertheless, data above this threshold became quite sparse, introducing large uncertainty. Considering that VOC/NOx ≈ 5.5 is often regarded as an approximate boundary for the VOC-sensitive regime of ozone formation (An et al., 2024), photochemical ON formation appears to be similarly promoted by VOCs elevation under VOC-limited to transitional conditions and then becomes suppressed when NOx is insufficient.

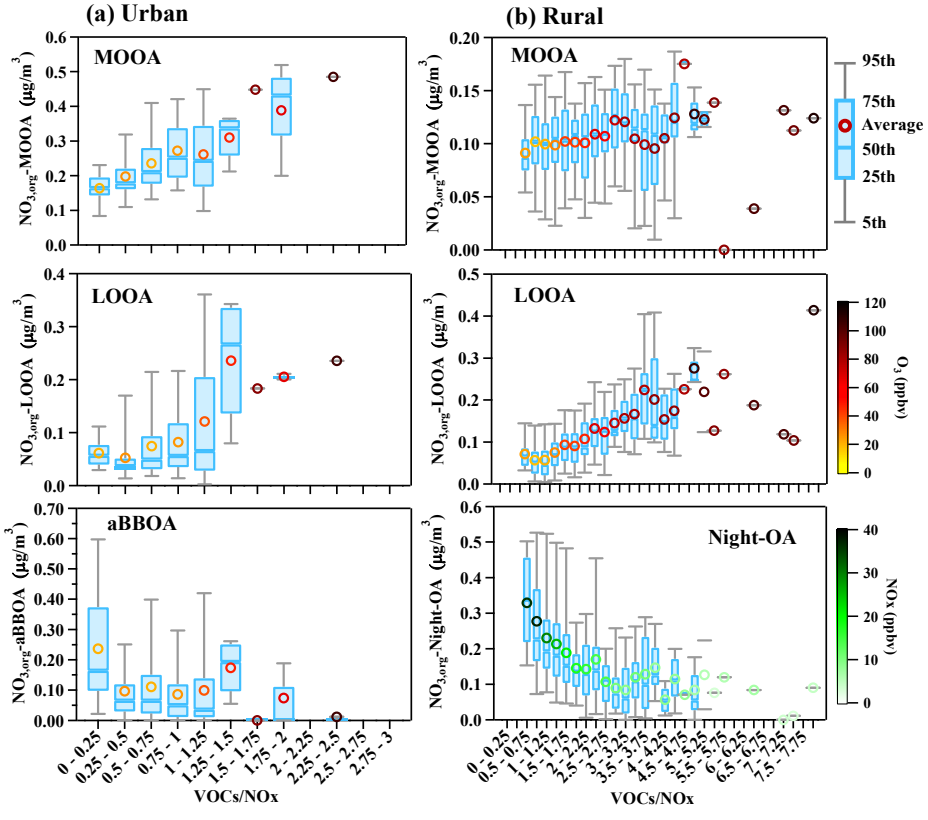

https://doi.org/10.5194/egusphere-2026-4552
Preprint. Discussion started: 25 August 2026

Figure 4: Boxplots of secondary organonitrates ($NO_{3,org}$) as a function of VOCs/NOx ratio at (a) urban and (b) rural sites. Organonitrates originated from daytime photochemical reactions were colored by O_3 concentration, while nighttime formation-related organonitrate (Night-OA) was colored by NOx concentration.

LOOA-related organonitrates were found to vary coupling with O_3 in a two-step covariation (Fig. 5), first increasing slowly at low O_3 concentrations (slope = 0.0004 urban, 0.0008 rural) and then rising sharply once O3 exceeded ~80 ppb (slope = 0.005 urban, 0.003 rural), with continuously increasing VOCs/NOx ratio. Mechanistically, under NOx-rich but VOC-limited conditions, the RO_2+NO reaction branches toward both O_3 and ON, with O_3 formation dominating. When O_3 reaches high levels, the increasing atmospheric oxidation capacity may enhance RO2 production, thereby accelerating ON formation in the presence of high VOC availability and sufficient NOx. The steeper slope at the urban site during the ON rapid increase phase suggests that higher urban NOx concentrations (21~29 ppb in urban vs. 9~13 ppb at the rural site) further promote ON photochemical formation under comparable oxidative conditions. Therefore, daytime ON formation via OH-initiated photochemical pathway generally increased with O_3 as well as the VOCs/NOx ratio, and may be further accelerated under high atmospheric oxidation capacity. However, because ON is a termination product of RO_2+NO pathway (Liebmann et al., 2019), i.e., interrupting the OH-RO_2-O_3-OH propagation cycle and temporarily storing NOx, enhanced ON formation might slow down the rise of ozone concentration, presenting an indirect inhibition effect. In Shanghai, a model study revealed that the similar inhibition effect on daytime O_3 formation by peroxy nitrates production could reach 16% (Li et al., 2025), which could be higher in those places (such as suburban areas) with lower NOx (Liu et al., 2021; Zeng et al., 2019).

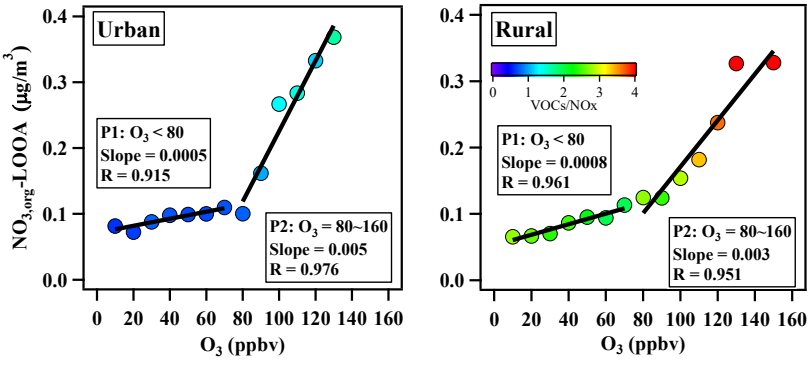

Figure 5: $NO_{3,org}$-LOOA as a function of O_3 (binned at 10 ppbv intervals) at urban (left) and rural (right) site. Dots are colored by VOCs/NOx ratio.

Conversely, the nocturnal formed ON, $NO_{3,org}$ associated with Night-OA, showed a distinct negative correlation with VOCs/NOx at the rural site, rapidly decreasing from 0.33 to 0.08 μg/m^3 as VOCs/NOx increased (Fig. 4b). This trend coincided with decreasing NOx concentrations, confirming that elevated NOx promotes ON nighttime formation through NO_3-initiated chemistry. The turning point for nocturnal case is about VOCs/NOx =3 (NOx =~10 ppb), after which $NO_{3,org}$-Night-OA waved at low level (~0.1). These results suggest that NOx availability, primarily by controlling NO_3 radical production through NO_2+O_3 reaction (Ng et al., 2017), played a dominant role in regulating nocturnal ON formation in the rural PRD.

Other secondary factors, including aBBOA at the urban site and MOOA as well as BBSOA (Fig. S15) at the rural site, exhibited

https://doi.org/10.5194/egusphere-2026-4552
Preprint. Discussion started: 25 August 2026

weaker or negligible correlations with VOCs/NOx ratio, suggesting their formation is less sensitive to local precursor balance. Overall, these findings demonstrate that the VOCs/NOx ratio modulates ON formation in a pathway-dependent manner. High VOC-to-NOx conditions favor daytime photochemical ON formation (LOOA and MOOA) within the VOC-sensitive regime (VOCs/NOx <5), while high NOx conditions (>10 ppb, VOC/NOx <3) enhance nocturnal ON production via NO_3-initiated chemistry. Elevated atmospheric oxidation capacity could further accelerate ON formation via OH-initiated pathway. The contrasting responses of source-resolved ON emphasize the importance of precursor balance in shaping ON formation regimes in the PRD.

3.5 Key VOC precursors in urban and rural regions

To further investigate the formation mechanism of secondary organonitrate, we estimated the production potential of gaseous ON from 55 measured VOCs via OH-, NO_3-, and O_3-initiated oxidation pathways, and the PP_{OH} and PP_{NO3} for all VOCs are showed in Fig. S16. Consistent with that total VOC concentrations were higher at the rural site (36.62 ppbv) than at the urban site (30.46 ppbv), the rural site exhibited higher total ON production potential (rural:0.18, urban: 0.06 ppbv/h), especially for the NO_3-initiated pathway. In contrast, OH-initiated PP_{ON} showed a narrower distribution (0~0.02 ppbv/h) range than the NO_3 pathway (0~0.04 ppbv/h), suggesting stronger variability of nocturnal chemistry and precursor reactivity.

Key VOCs were identified for ON formation potential via three pathways as shown in Fig. 6 with more details in Fig. S17. Via photochemical formation pathway initiated by OH radical, 8 predominant VOCs accounted for around 80% of total PP_{OH}. Among them, n-Pentane, monoterpenes, isoprene, and m,p-xylene were the dominant contributors at both sites, although their relative importance differed substantially. At the urban site, n-pentane was the largest contributor to PP_{OH} (19.4%), reflecting the importance of traffic-related emissions because it was mainly emitted from gasoline evaporation and vehicle exhaust, and has previously been identified as an important precursor of alkyl nitrates in China (Sun et al., 2018; Zhang et al., 2019). In contrast, m,p-xylene dominated rural PP_{OH} (22.2%), tightly followed by n-pentane (21.8%), likely reflecting regional transport of industrial and urban pollutants including vehicle exhausts from the central PRD (Ling et al., 2011). The concentration of m/p-xylene at the rural site (3.89 ppbv) was nearly four times that at the urban site (1.02 ppbv), consistent with downwind transport of aromatic VOCs.

Isoprene and monoterpenes together accounted for 33.6% and 19.4% of PP_{OH} at the urban and rural sites, respectively, comparable with values reported in Bakersfield (~29%) (Rollins et al., 2013) and Finnish boreal forest (31%)(Liebmann et al., 2019) . The remarkable contribution of isoprene likely reflects strong BVOC emissions under the warm subtropical climate of the PRD. However, monoterpenes at the urban site of Guangzhou were likely influenced by anthropogenic emissions such as volatile chemical products (VCPs) as identified in previous study (Li et al., 2022). In the present study, the anthropogenic source of monoterpene in urban Guangzhou is supported by the good correlation with CO (R = 0.60), whereas weaker correlation at the rural site (R = 0.21) suggests stronger biogenic influence there.

https://doi.org/10.5194/egusphere-2026-4552
Preprint. Discussion started: 25 August 2026

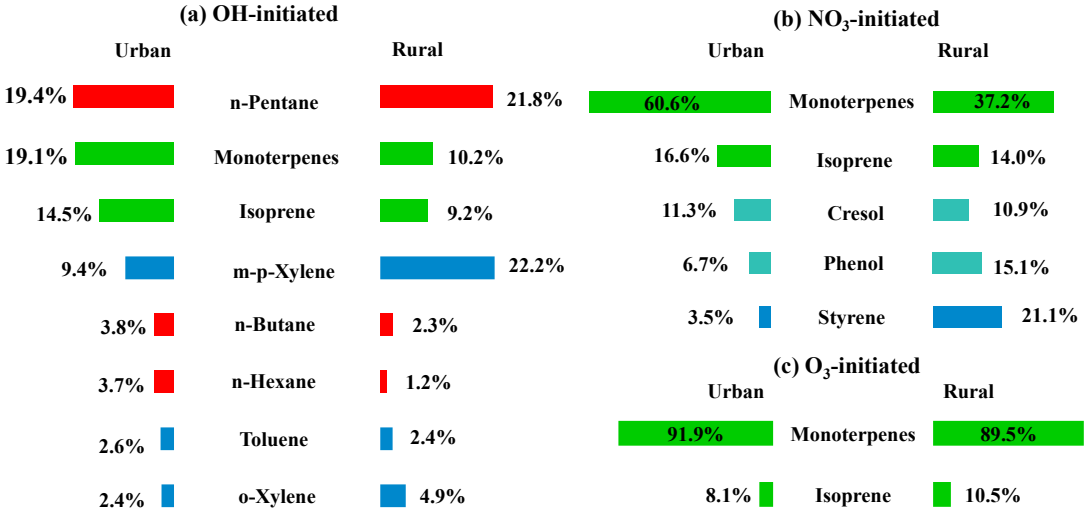

Figure 6: Contribution to total PP_{ON} from ON formed via (a) OH-initiated, (b) NO_3-initiated and (c) O_3-initiated pathways at urban and rural sites.

Compared with OH chemistry, ON formation via the NO_3 pathway was dominated by fewer (five) but more reactive VOCs. Monoterpenes were the largest contributor to PP_{NO3} at both sites (60.6% urban and 37.2% rural), consistent with previous observations in Shenzhen(Yu et al., 2019). However, anthropogenic benzene-containing VOCs played a much larger role at the rural site. Styrene alone contributed 21.1% of rural PP_{NO3} because of its high NO_3 reactivity (Lin et al., 2022), while phenol and cresol together accounted for 26.0%. These phenolic VOCs are mainly associated with combustion emissions and biomass burning (Ren et al., 2025), supporting the source apportionment results in Section 3.3 that BB-related emissions contributed to ON not only directly but also through secondary oxidation of BB-emitted VOC precursors. Overall, anthropogenic VOCs (styrene, phenol, and cresol) contributed comparably to biogenic VOCs (isoprene and monoterpenes) for nighttime ON formation at the rural site (47.1% vs. 51.2%), indicating substantial human influence on ON chemistry even in the rural PRD. For O_3-initialed pathway, monoterpenes were overwhelming contributor to PP_{O3} at both sites, accounting for about 90% of ON formation potential. When all three pathways were combined (Fig. 7b, e), monoterpenes remained the largest single VOC class contributing to PP_{ON} at both sites (28~39%), while aromatic and phenolic VOCs became the dominant group at the rural site (41%), and anthropogenic VOCs contributed more than half (59%). These results highlight the complexity of ON formation in regions characterized by both intensive anthropogenic emissions and abundant subtropical vegetation.

The diurnal variation of accumulated PP_{ON} from OH-, NO_3-, and O_3-initiated pathways further illustrated their contributions in a whole day (Fig. 7a, d). O_3-initiated oxidation contributed only a small fraction (4–8%, Fig. 7c, f) at both sites. At the urban site, OH chemistry dominated ON production (~58%), and PP_{ON} exhibited a pronounced daytime peak consistent with LOOA- and MOOA-related ON, although the particulate ON peak lagged behind gaseous PP_{ON} peak by 2–3 h, likely due to gas-particle partitioning processes slowed under higher daytime temperature conditions. In contrast, NO_3 chemistry dominated total PP_{ON} at the rural site (55%), producing a distinct early-evening peak comparable to the daytime maximum. This feature

https://doi.org/10.5194/egusphere-2026-4552
Preprint. Discussion started: 25 August 2026

was broadly consistent with the observed diurnal variations of Night-OA and BBSOA-related ON. On average, nighttime PP_{NO3} at the rural site was much higher than that at the urban site (0.13 vs. 0.02 ppbv/h), suggesting substantial nighttime NO_3 chemistry in the rural area. This is reasonable because lower NO concentrations at the rural site reduced NO_3 radical titration and favored NO_3 accumulation (Asaf et al., 2009; Brown et al., 2016; Wang et al., 2020), while elevated nighttime O_3 and NO_2 levels in the PRD further promoted NO_3 production (Yu et al., 2020). Together with abundant aromatic from industry and cities, as well as BB-related VOCs, these conditions favored efficient nocturnal ON formation. The potentially significant contribution of anthropogenic VOCs to ON may help explain the missing source revealed in a model study, which found that known chemistry only accounted for only one-third of the observed organonitrates (Kenagy et al., 2021). Overall, the coexistence of abundant anthropogenic VOCs, biomass-burning emissions, and strong subtropical BVOC emissions makes the PRD highly favorable for both daytime and nocturnal ON formation.

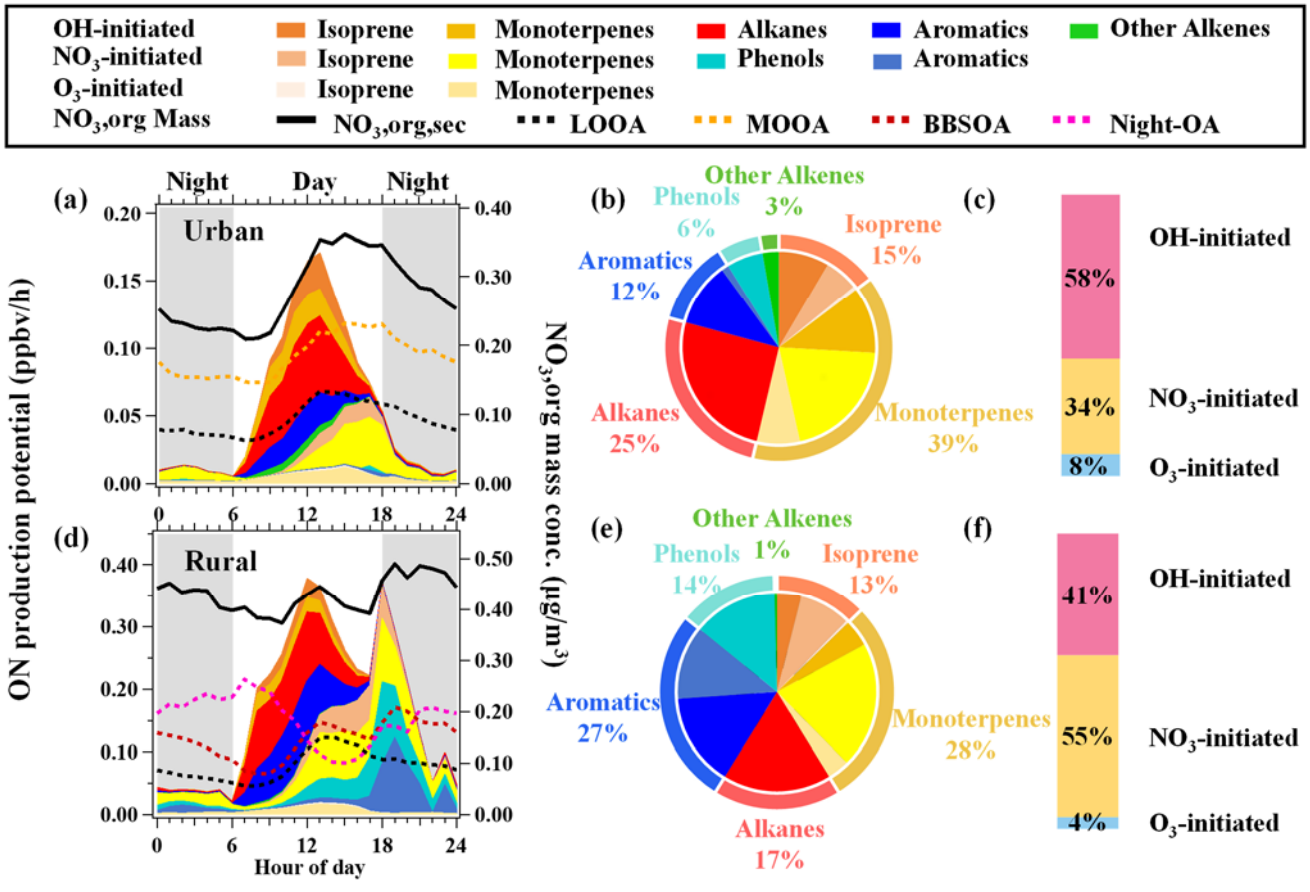

Figure 7: Contribution of OH-(during daytime) and NO_3-initiated (during nighttime, considering brunching ration) production degradation of VOCs to the formation of organonitrates in (c) urban and (d) rural site, respectively.

3.6 Refractory ON associated with nighttime and BB processes

Using the PMF method, pON associated with refractory components could also be extracted from SP-AMS measurements in

https://doi.org/10.5194/egusphere-2026-4552
Preprint. Discussion started: 25 August 2026

laser-on mode ($PMF_{org+Cx+NOx}$, more details in TextS1 and Figs S6-9). On average, the $NO_{3,org}$ mass concentrations derived from laser-on mode (urban: 0.68 μg m^{-3}; rural: 1.25 μg m^{-3}) were higher than those from laser-off mode (urban: 0.56 μg m^{-3}; rural: 0.65 μg m^{-3}). Figure 8 shows the difference in source-resolved $NO_{3,org}$ between laser-on and laser-off modes ($\Delta NO_{3,org}$), which is interpreted here as refractory ON associated with BC-coating particles.

Compared with the urban site, refractory ON was much more pronounced at the rural site. In urban Guangzhou, $\Delta NO_{3,org}$ associated with different sources were quite close to zero, with the maximum increment only 0.04 μg m^{-3}, related to aged BB emissions. In contrast, substantial enhancement of refractory ON was observed in the rural PRD, mainly associated with BBOA and Night-OA. The $\Delta NO_{3,org}$ linked to these two factors was 3.8 and 1.2 times higher, respectively, than the corresponding non-refractory ON. Together, BBOA- and Night-OA-related refractory ON accounted for more than 70% of total $\Delta NO_{3,org}$ in the rural atmosphere (43% and 30%, respectively, after accounting for the negative contribution from MOOA). These results indicate that biomass combustion emissions and BB-influenced nocturnal chemistry contributed substantially to refractory pON in rural PRD.

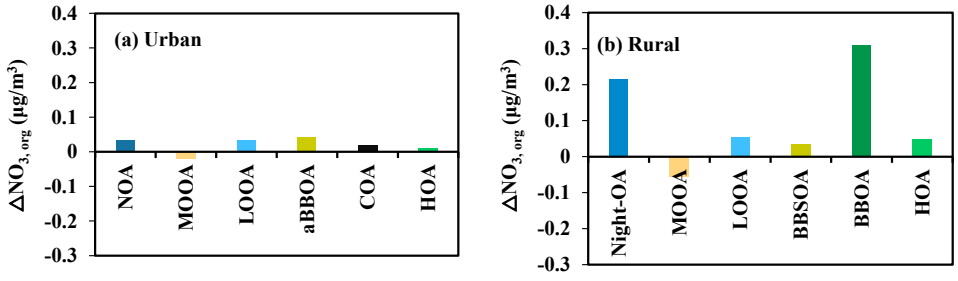

Figure 8: Differences between source-resolved NO3,org mass concentrations with laser on and off at urban (left) and rural (right) sites.

The distinct refractory signal associated with BBOA and Night-OA also supports the formation mechanisms proposed in Sections 3.3 and 3.5. Nighttime ON formation at the rural site was strongly linked to BB emissions and NO_3-initiated oxidation. Biomass burning emitted abundant aromatic and phenolic precursors (Ren et al., 2025), which can undergo rapid oxidation and nitration to form low-volatility organic nitrogen compounds. Previous studies have shown that BrC particles and tar-ball-like material emitted from incomplete combustion can contain substantial amounts of nitrogen-containing chromophores, including organonitrates and nitro-aromatics, contributing significantly to aerosol light absorption (Adachi et al., 2019; Corbin et al., 2019; Lin et al., 2017; Wu et al., 2024b) . The enhanced refractory ON associated with Night-OA further suggests that part of the nocturnal secondary products was likely formed on or condensed onto refractory BC/BrC-containing particles during nighttime aging processes. By comparison, $\Delta NO_{3,org}$ associated with LOOA, HOA and aBBOA showed negligible amount, suggesting that these components are mainly non-refractory. Slightly negative $\Delta NO_{3,org}$ related to MOOA at both sites was probably caused by the PMF uncertainties when fitting two datasets (from two modes) separately. Nevertheless, the clear enhancement of refractory ON at the rural site demonstrates that refractory particles related with BB and nocturnal process can represent an important but previously under-characterized carrier of atmospheric ON, which cannot be effectively resolved

https://doi.org/10.5194/egusphere-2026-4552
Preprint. Discussion started: 25 August 2026

by conventional AMS without SP mode.

4.Conclusion

This study characterized pON at urban and rural sites in the PRD using SP-AMS measurements during autumn. The PMF method showed better agreement with independent FIGAERO-CIMS measurements than the NOx ratio method, and was therefore selected for pON quantification and source analysis. Average pON mass concentration was slightly higher at the rural site than at the urban site, whereas the contribution of $NO_{3,org}$ to total nitrate was comparable at both sites. The observed concentrations were within the range previously reported from AMS measurements, but their source-resolved characteristics differed substantially between the urban and rural sites.

In urban Guangzhou, pON was mainly associated with daytime photochemical formation and regional aging processes (49%). In contrast, nocturnal formation contributed substantially at the rural site (29%). BB-related emissions also had important impact on pON at both sites (25% and 34%, respectively). As indicated by the relationships with VOCs/NOx ratios, daytime photochemical ON formation was enhanced under elevated VOC availability, whereas nighttime formation was favored under NOx-rich conditions.

Major VOC precursors for PP_{ON} were broadly similar at both sites, with monoterpenes, isoprene, alkanes, and aromatics dominating OH-initiated ON formation (80%), while monoterpenes, styrene, isoprene and aromatic VOCs were the major contributors to NO_3-initiated production. Anthropogenic VOCs contributed substantially to the estimated-ON production potential especially at the rural site (59%), indicating that human activities strongly influenced ON chemistry even outside urban centers. Notably, refractory ON associated with BBOA and Night-OA was observed at the rural site, but negligible at the urban site, suggesting that BB and nighttime processes may contribute to refractory ON associated with BC/BrC-containing particles.

Overall, pON formation in the PRD was jointly controlled by photochemistry, nighttime NO_3 chemistry, biomass burning, and anthropogenic emissions, with clear urban-rural contrasts. Our results suggest that although the dominance of SOA-related ON was consistent at the urban and rural sites, and with findings of observations in other areas, the relative importance of individual secondary processes varied among different atmospheric environments. The substantial contributions of nighttime and refractory ON highlight the complexity of ON chemistry in anthropogenically influence subtropical environments and warrant further investigation.

Several limitations should be considered. Source-resolved ON is subject to uncertainties associated with PMF factor separation and spectral interpretation. The PPON calculation was limited to 55 measured VOCs and did not account for gas-particle partitioning, chemical loss, deposition, or other formation processes. Thus, it represents relative importance of different precursors and pathways rather than ambient pON concentrations. In addition, although the laser-on/off comparison indicates a refractory ON fraction, SP-AMS cannot determine its molecular composition or exact mixing state. Future measurements combining SP-AMS with molecular-level characterization and more comprehensive VOC measurements are needed to better

https://doi.org/10.5194/egusphere-2026-4552
Preprint. Discussion started: 25 August 2026

constrain refractory ON and nighttime ON chemistry and improve their representation in atmospheric models.

Data availability

The datasets supporting the findings of this study are publicly available at https://doi.org/10.17632/b57cffj2kf.1 (Huang, 2026).

Supplement link

The supplement related to this article is available online at:

Author contributions

SH conceived and led this research. SH, WH, BY, MS and XW designed the experiments. SH, QS, WL and YK conducted the experiments. SH and LW wrote the manuscript. SH, LW, YL, YK, performed the data analysis. YP, SY, MC, DC, YD and WS provided data from external instruments and model simulation. WH and YK provided insights into data analysis. SH, BY, MS and XW secured fundings. All the authors contributed to revisions of this paper.

Competing interests

I declare that I or my co-authors have competing interests as follows: At least one of the (co-)authors is a member of the editorial board of Atmospheric Chemistry and Physics.

Financial support

This work is supported by the National Natural Science Foundation of China (grant nos. 42377088 and 41807302), the National Key Research and Development Program of China (grant nos. 2023YFC3706204 and 2016YFC0202206), Guangdong Natural Science Foundation (grant no. 2018A030313384), Key-Area Research and Development Program of Guangdong Province (grant no. 2019B110206001), Special Fund Project for Science and Technology Innovation Strategy of Guangdong Province (grant no. 2019B121205004), and Guangdong Natural Science Funds for Distinguished Young Scholar (grant no. 2018B030306037).

References

Adachi K., Sedlacek, A. J., 3rd, Kleinman, L., Springston, S. R., Wang, J., Chand, D., Hubbe, J. M., Shilling, J. E., Onasch, T. B., Kinase, T., Sakata, K., Takahashi, Y., and Buseck, P. R.: Spherical tarball particles form through rapid chemical and physical

https://doi.org/10.5194/egusphere-2026-4552
Preprint. Discussion started: 25 August 2026

changes of organic matter in biomass-burning smoke, Proc Natl Acad Sci U S A, 116, 19336-19341, doi:10.1073/pnas.1900129116, 2019.

Ahern A., Robinson, E., Tkacik, D., Saleh, R., Hatch, L., Barsanti, K., Stockwell, C., Yokelson, R., Presto, A., and Robinson, A.: Production of secondary organic aerosol during aging of biomass burning smoke from fresh fuels and its relationship to VOC precursors, Journal of Geophysical Research: Atmospheres, 124, 3583-3606, 2019.

Albinet A., Leoz-Garziandia, E., Budzinski, H., Villenave, E., and Jaffrezo, J. L.: Nitrated and oxygenated derivatives of polycyclic aromatic hydrocarbons in the ambient air of two French alpine valleysPart 1: Concentrations, sources and gas/particle partitioning, Atmospheric Environment, 42, 43-54, doi:10.1016/j.atmosenv.2007.10.009, 2008.

An T., Li, J., Lin, Q., and Li, G.: Ozone formation potential related to the release of volatile organic compounds (VOCs) and nitrogen oxide (NOX) from a typical industrial park in the Pearl River Delta, Environmental Science: Atmospheres, 4, 1229-1238, doi:10.1039/d4ea00091a, 2024.

Andersen S. T., Sander, R., Dewald, P., Wüst, L., Seubert, T., Türk, G. N. T. E., Schuladen, J., McGillen, M. R., Xue, C., Mellouki, A., Kukui, A., Michoud, V., Cirtog, M., Cazaunau, M., Bauville, A., Bouzidi, H., Formenti, P., Denjean, C., Etienne, J. C., Garrouste, O., Cantrell, C., Lelieveld, J., and Crowley, J. N.: Short-lived organic nitrates in a suburban temperate forest: an indication of efficient assimilation of reactive nitrogen by the biosphere?, Atmos. Chem. Phys., 25, 5893-5909, doi:10.5194/acp-25-5893-2025, 2025.

Asaf D., Pedersen, D., Matveev, V., Peleg, M., Kern, C., Zingler, J., Platt, U., and Luria, M.: Long-term measurements of NO3 radical at a semiarid urban site: 1. Extreme concentration events and their oxidation capacity, Environmental science & technology 43, 9117-9123, 2009.

Ayres B. R., Allen, H. M., Draper, D. C., Brown, S. S., Wild, R. J., Jimenez, J. L., Day, D. A., Campuzano-Jost, P., Hu, W., de Gouw, J., Koss, A., Cohen, R. C., Duffey, K. C., Romer, P., Baumann, K., Edgerton, E., Takahama, S., Thornton, J. A., Lee, B. H., Lopez-Hilfiker, F. D., Mohr, C., Wennberg, P. O., Nguyen, T. B., Teng, A., Goldstein, A. H., Olson, K., and Fry, J. L.: Organic nitrate aerosol formation via NO3 + biogenic volatile organic compounds in the southeastern United States, Atmospheric Chemistry and Physics, 15, 13377-13392, doi:10.5194/acp-15-13377-2015, 2015.

Bertman S. B., Roberts, J. M., Parrish, D. D., Buhr, M. P., Goldan, P. D., Kuster, W. C., Fehsenfeld, F. C., Montzka, S. A., and Westberg, H.: Evolution of alkyl nitrates with air mass age, Journal of Geophysical Research: Atmospheres, 100, 22805-22813, 1995.

Bertrand A., Stefenelli, G., Jen, C. N., Pieber, S. M., Bruns, E. A., Temime-Roussel, B., Slowik, J. G., Goldstein, A. H., El Haddad, I., Baltensperger, U., Prévôt, A. S. H., Wortham, H., and Marchand, N.: Evolution of the chemical fingerprint of biomass burning organic aerosol during aging, Atmos. Chem. Phys. Discuss., 2018, 1-33, doi:10.5194/acp-2017-1196, 2018.

Boyd C. M., Sanchez, J., Xu, L., Eugene, A. J., Nah, T., Tuet, W. Y., Guzman, M. I., and Ng, N. L.: Secondary organic aerosol formation from the β-pinene+NO3 system: effect of humidity and peroxy radical fate, Atmospheric Chemistry and Physics, 15, 7497-7522, doi:10.5194/acp-15-7497-2015, 2015.

https://doi.org/10.5194/egusphere-2026-4552
Preprint. Discussion started: 25 August 2026

Brito J., Freney, E., Dominutti, P., Borbon, A., Haslett, S. L., Batenburg, A. M., Colomb, A., Dupuy, R., Denjean, C., and Burnet, F.: Assessing the role of anthropogenic and biogenic sources on PM 1 over southern West Africa using aircraft measurements, Atmospheric Chemistry and Physics, 18, 757-772, 2018.

Brown S. S., Dubé, W. P., Tham, Y. J., Zha, Q., Xue, L., Poon, S., Wang, Z., Blake, D. R., Tsui, W., and Parrish, D. D.: Nighttime chemistry at a high altitude site above Hong Kong, Journal of Geophysical Research: Atmospheres, 121, 2457-2475, 2016.

Bruns E. A., Perraud, V., Zelenyuk, A., Ezell, M. J., Johnson, S. N., Yu, Y., Imre, D., Finlayson-Pitts, B. J., and Alexander, M. L.: Comparison of FTIR and particle mass spectrometry for the measurement of particulate organic nitrates, Environmental science & technology, 44, 1056-1061, 2010.

Cai Y., Ye, C., Chen, W., Hu, W., Song, W., Peng, Y., Huang, S., Qi, J., Wang, S., Wang, C., Wu, C., Wang, Z., Wang, B., Huang, X., He, L., Gligorovski, S., Yuan, B., Shao, M., and Wang, X.: The important contribution of secondary formation and biomass burning to oxidized organic nitrogen (OON) in a polluted urban area: insights from in situ measurements of a chemical ionization mass spectrometer (CIMS), Atmos. Chem. Phys., 23, 8855-8877, doi:10.5194/acp-23-8855-2023, 2023.

Chang Y., Gao, Y., Lu, Y., Qiao, L., Kuang, Y., Cheng, K., Wu, Y., Lou, S., Jing, S., Wang, H., and Huang, C.: Discovery of a Potent Source of Gaseous Amines in Urban China, Environmental Science & Technology Letters, 8, 725-731, doi:10.1021/acs.estlett.1c00229, 2021.

Corbin J. C., Czech, H., Massabò, D., de Mongeot, F. B., Jakobi, G., Liu, F., Lobo, P., Mennucci, C., Mensah, A. A., and Orasche, J.: Infrared-absorbing carbonaceous tar can dominate light absorption by marine-engine exhaust, Npj Climate and Atmospheric Science, 2, 1-10, 2019.

Day D. A., Campuzano-Jost, P., Nault, B. A., Palm, B. B., Hu, W., Guo, H., Wooldridge, P. J., Cohen, R. C., Docherty, K. S., Huffman, J. A., de Sá, S. S., Martin, S. T., and Jimenez, J. L.: A systematic re-evaluation of methods for quantification of bulk particle-phase organic nitrates using real-time aerosol mass spectrometry, Atmos. Meas. Tech., 15, 459-483, doi:10.5194/amt-15-459-2022, 2022.

Ditto J. C., Joo, T., Slade, J. H., Shepson, P. B., Ng, N. L., and Gentner, D. R.: Nontargeted Tandem Mass Spectrometry Analysis Reveals Diversity and Variability in Aerosol Functional Groups across Multiple Sites, Seasons, and Times of Day, Environmental Science & Technology Letters, 7, 60-69, doi:10.1021/acs.estlett.9b00702, 2020.

Duan F., Liu, X., Yu, T., and Cachier, H.: Identification and estimate of biomass burning contribution to the urban aerosol organic carbon concentrations in Beijing, Atmospheric Environment, 38, 1275-1282, doi:10.1016/j.atmosenv.2003.11.037, 2004.

Fang Z., Deng, W., Zhang, Y., Ding, X., Tang, M., Liu, T., Hu, Q., Zhu, M., Wang, Z., Yang, W., Huang, Z., Song, W., Bi, X., Chen, J., Sun, Y., George, C., and Wang, X.: Open burning of rice, corn and wheat straws: primary emissions, photochemical aging, and secondary organic aerosol formation, Atmospheric Chemistry and Physics, 17, 14821-14839, doi:10.5194/acp-17-14821-2017, 2017.

https://doi.org/10.5194/egusphere-2026-4552
Preprint. Discussion started: 25 August 2026

Farmer D. K., Matsunaga, A., Docherty, K. S., Surratt, J. D., Seinfeld, J. H., Ziemann, P. J., and Jimenez, J. L.: Response of an aerosol mass spectrometer to organonitrates and organosulfates and implications for atmospheric chemistry, Proc Natl Acad Sci U S A, 107, 6670-6675, doi:10.1073/pnas.0912340107, 2010.

Farmer D. K., Perring, A. E., Wooldridge, P. J., Blake, D. R., Baker, A., Meinardi, S., Huey, L. G., Tanner, D., Vargas, O., and Cohen, R. C.: Impact of organic nitrates on urban ozone production, Atmos. Chem. Phys., 11, 4085-4094, doi:10.5194/acp-11-4085-2011, 2011.

Fernández P., Grifoll, M., Solanas, A. M., Bayona, J. M., and Albalgés1, J.: Bioassay-directed chemical analysis of genotoxic components in coastal sediments, Environmental science & technology, 26, 817-829, 1992.

Fry J. L., Draper, D. C., Zarzana, K. J., Campuzano-Jost, P., Day, D. A., Jimenez, J. L., Brown, S. S., Cohen, R. C., Kaser, L., Hansel, A., Cappellin, L., Karl, T., Hodzic Roux, A., Turnipseed, A., Cantrell, C., Lefer, B. L., and Grossberg, N.: Observations of gas- and aerosol-phase organic nitrates at BEACHON-RoMBAS 2011, Atmospheric Chemistry and Physics, 13, 8585-8605, doi:10.5194/acp-13-8585-2013, 2013.

Gaston C. J., Lopez-Hilfiker, F. D., Whybrew, L. E., Hadley, O., McNair, F., Gao, H., Jaffe, D. A., and Thornton, J. A.: Online molecular characterization of fine particulate matter in Port Angeles, WA: Evidence for a major impact from residential wood smoke, Atmospheric Environment, 138, 99-107, doi:10.1016/j.atmosenv.2016.05.013, 2016.

Ge D., Nie, W., Sun, P., Liu, Y., Wang, T., Wang, J., Wang, J., Wang, L., Zhu, C., Wang, R., Liu, T., Chi, X., and Ding, A.: Characterization of particulate organic nitrates in the Yangtze River Delta, East China, using the time-of-flight aerosol chemical speciation monitor, Atmos. Environ., 272, 118927, doi:https://doi.org/10.1016/j.atmosenv.2021.118927, 2022.

George C., Ammann, M., D'Anna, B., Donaldson, D. J., and Nizkorodov, S. A.: Heterogeneous photochemistry in the atmosphere, Chem Rev, 115, 4218-4258, doi:10.1021/cr500648z, 2015.

George I. J., and Abbatt, J. P.: Heterogeneous oxidation of atmospheric aerosol particles by gas-phase radicals, Nat Chem, 2, 713-722, doi:10.1038/nchem.806, 2010.

Hayes P. L., Ortega, A. M., Cubison, M. J., Froyd, K. D., Zhao, Y., Cliff, S. S., Hu, W. W., Toohey, D. W., Flynn, J. H., Lefer, B. L., Grossberg, N., Alvarez, S., Rappenglück, B., Taylor, J. W., Allan, J. D., Holloway, J. S., Gilman, J. B., Kuster, W. C., de Gouw, J. A., Massoli, P., Zhang, X., Liu, J., Weber, R. J., Corrigan, A. L., Russell, L. M., Isaacman, G., Worton, D. R., Kreisberg, N. M., Goldstein, A. H., Thalman, R., Waxman, E. M., Volkamer, R., Lin, Y. H., Surratt, J. D., Kleindienst, T. E., Offenberg, J. H., Dusanter, S., Griffith, S., Stevens, P. S., Brioude, J., Angevine, W. M., and Jimenez, J. L.: Organic aerosol composition and sources in Pasadena, California, during the 2010 CalNex campaign, J. Geophys. Res. - Atmos., 118, 9233-9257, doi:10.1002/jgrd.50530, 2013.

Hou X., Chan, C. K., Dong, G. H., and Yim, S. H. L.: Impacts of transboundary air pollution and local emissions on PM2.5 pollution in the Pearl River Delta region of China and the public health, and the policy implications, Environmental Research Letters, 14, doi:10.1088/1748-9326/aaf493, 2019.

Huang S.: Urban and rural organonitrate in PM1 in PRD, Mendeley Data (data set), doi:10.17632/b57cffj2kf.1, 2026.

https://doi.org/10.5194/egusphere-2026-4552
Preprint. Discussion started: 25 August 2026

Huang W., Yang, Y., Wang, Y., Gao, W., Li, H., Zhang, Y., Li, J., Zhao, S., Yan, Y., Ji, D., Tang, G., Liu, Z., Wang, L., Zhang, R., and Wang, Y.: Exploring the inorganic and organic nitrate aerosol formation regimes at a suburban site on the North China Plain, Sci Total Environ, 768, 144538, doi:10.1016/j.scitotenv.2020.144538, 2021.

Joo T., Rivera-Rios, J. C., Takeuchi, M., Alvarado, M. J., and Ng, N. L.: Secondary Organic Aerosol Formation from Reaction of 3-Methylfuran with Nitrate Radicals, ACS Earth and Space Chemistry, 3, 922-934, doi:10.1021/acsearthspacechem.9b00068, 2019.

Kenagy H. S., Romer Present, P. S., Wooldridge, P. J., Nault, B. A., Campuzano-Jost, P., Day, D. A., Jimenez, J. L., Zare, A., Pye, H. O. T., Yu, J., Song, C. H., Blake, D. R., Woo, J. H., Kim, Y., and Cohen, R. C.: Contribution of Organic Nitrates to Organic Aerosol over South Korea during KORUS-AQ, Environ Sci Technol, 55, 16326-16338, doi:10.1021/acs.est.1c05521, 2021.

Kenagy H. S., Sparks, T. L., Wooldridge, P. J., Weinheimer, A. J., Ryerson, T. B., Blake, D. R., Hornbrook, R. S., Apel, E. C., and Cohen, R. C.: Evidence of Nighttime Production of Organic Nitrates During SEAC4RS, FRAPPÉ, and KORUS-AQ, Geophys. Res. Lett., 47, e2020GL087860, doi:10.1029/2020gl087860, 2020.

Kiendler-Scharr A., Mensah, A. A., Friese, E., Topping, D., Nemitz, E., Prevot, A. S. H., Äijälä, M., Allan, J., Canonaco, F., Canagaratna, M., Carbone, S., Crippa, M., Dall Osto, M., Day, D. A., De Carlo, P., Di Marco, C. F., Elbern, H., Eriksson, A., Freney, E., Hao, L., Herrmann, H., Hildebrandt, L., Hillamo, R., Jimenez, J. L., Laaksonen, A., McFiggans, G., Mohr, C., O'Dowd, C., Otjes, R., Ovadnevaite, J., Pandis, S. N., Poulain, L., Schlag, P., Sellegri, K., Swietlicki, E., Tiitta, P., Vermeulen, A., Wahner, A., Worsnop, D., and Wu, H. C.: Ubiquity of organic nitrates from nighttime chemistry in the European submicron aerosol, Geophys. Res. Lett., 43, 7735-7744, doi:10.1002/2016GL069239, 2016.

Kuang Y., Huang, S., Xue, B., Luo, B., Song, Q., Chen, W., Hu, W., Li, W., Zhao, P., Cai, M., Peng, Y., Qi, J., Li, T., Wang, S., Chen, D., Yue, D., Yuan, B., and Shao, M.: Contrasting effects of secondary organic aerosol formations on organic aerosol hygroscopicity, Atmos. Chem. Phys., 21, 10375-10391, doi:10.5194/acp-21-10375-2021, 2021.

Kuang Y., Luo, B., Huang, S., Liu, J., Hu, W., Peng, Y., Chen, D., Yue, D., Xu, W., Yuan, B., and Shao, M.: Formation of highly absorptive secondary brown carbon through nighttime multiphase chemistry of biomass burning emissions, Atmos. Chem. Phys., 25, 3737-3752, doi:10.5194/acp-25-3737-2025, 2025.

Lalchandani V., Srivastava, D., Dave, J., Mishra, S., Tripathi, N., Shukla, A. K., Sahu, R., Thamban, N. M., Gaddamidi, S., Dixit, K., Ganguly, D., Tiwari, S., Srivastava, A. K., Sahu, L., Rastogi, N., Gargava, P., and Tripathi, S. N.: Effect of Biomass Burning on PM 2.5 Composition and Secondary Aerosol Formation During Post-Monsoon and Winter Haze Episodes in Delhi, Journal of Geophysical Research: Atmospheres, 127, doi:10.1029/2021jd035232, 2021.

Lanz V. A., Alfarra, M. R., Baltensperger, U., Buchmann, B., Hueglin, C., and Prévôt, A. S. H.: Source apportionment of submicron organic aerosols at an urban site by factor analytical modelling of aerosol mass spectra, Atmospheric Chemistry and Physics, 7, 1503-1522, doi:10.5194/acp-7-1503-2007, 2007.

Le Breton M., Psichoudaki, M., Hallquist, M., Watne, Å. K., Lutz, A., and Hallquist, Å. M.: Application of a FIGAERO ToF

https://doi.org/10.5194/egusphere-2026-4552
Preprint. Discussion started: 25 August 2026

CIMS for on-line characterization of real-world fresh and aged particle emissions from buses, Aerosol Sci. Tech., 53, 244-259, doi:10.1080/02786826.2019.1566592, 2019.

Lee A. K. Y., Abbatt, J. P. D., Leaitch, W. R., Li, S.-M., Sjostedt, S. J., Wentzell, J. J. B., Liggio, J., and Macdonald, A. M.: Substantial secondary organic aerosol formation in a coniferous forest: observations of both day- and nighttime chemistry, Atmospheric Chemistry and Physics, 16, 6721-6733, doi:10.5194/acp-16-6721-2016, 2016a.

Lee A. K. Y., Adam, M. G., Liggio, J., Li, S. M., Li, K., Willis, M. D., Abbatt, J. P. D., Tokarek, T. W., Odame-Ankrah, C. A., Osthoff, H. D., Strawbridge, K., and Brook, J. R.: A large contribution of anthropogenic organo-nitrates to secondary organic aerosol in the Alberta oil sands, Atmos. Chem. Phys., 19, 12209-12219, doi:10.5194/acp-19-12209-2019, 2019.

Lee B. H., Mohr, C., Lopez-Hilfiker, F. D., Lutz, A., Hallquist, M., Lee, L., Romer, P., Cohen, R. C., Iyer, S., Kurtén, T., Hu, W., Day, D. A., Campuzano-Jost, P., Jimenez, J. L., Xu, L., Ng, N. L., Guo, H., Weber, R. J., Wild, R. J., Brown, S. S., Koss, A., de Gouw, J., Olson, K., Goldstein, A. H., Seco, R., Kim, S., McAvey, K., Shepson, P. B., Starn, T., Baumann, K., Edgerton, E. S., Liu, J., Shilling, J. E., Miller, D. O., Brune, W., Schobesberger, S., D'Ambro, E. L., and Thornton, J. A.: Highly functionalized organic nitrates in the southeast United States: Contribution to secondary organic aerosol and reactive nitrogen budgets, P. Natl. Acad. Sci. USA, 113, 1516-1521, doi:10.1073/pnas.1508108113, 2016b.

Lee L., Wooldridge, P., Degouw, J., Brown, S., Bates, T., Quinn, P., Cohen, R. J. A. C., and Physics: Particulate organic nitrates observed in an oil and natural gas production region during wintertime, Atmospheric Chemistry and Physics, 15, 9313-9325, 2015.

Li C., Chen, X., Wang, H., Zhai, T., Ma, X., Yang, X., Chen, S., Zhou, M., Lou, S., Li, X., Zeng, L., and Lu, K.: The impact of organic nitrates on summer ozone formation in Shanghai, China, Atmos. Chem. Phys., 25, 3905-3918, doi:10.5194/acp-25-3905-2025, 2025.

Li X. B., Yuan, B., Wang, S., Wang, C., Lan, J., Liu, Z., Song, Y., He, X., Huangfu, Y., Pei, C., Cheng, P., Yang, S., Qi, J., Wu, C., Huang, S., You, Y., Chang, M., Zheng, H., Yang, W., Wang, X., and Shao, M.: Variations and sources of volatile organic compounds (VOCs) in urban region: insights from measurements on a tall tower, Atmos. Chem. Phys., 22, 10567-10587, doi:10.5194/acp-22-10567-2022, 2022.

Liao Y., Yu, M., Liang, L., Wang, X., Yin, J., Fang, Z., Chang, M., Yuan, B., Shao, M., and Huang, S.: Sources and characteristic components of atmospheric organic aerosols in the autumn suburbs of Guangzhou, China Environmental Sciences, 46, 53-65, 2026.

Liebmann J., Sobanski, N., Schuladen, J., Karu, E., Hellén, H., Hakola, H., Zha, Q., Ehn, M., Riva, M., Heikkinen, L., Williams, J., Fischer, H., Lelieveld, J., and Crowley, J. N.: Alkyl nitrates in the boreal forest: formation via the NO3-, OH- and O3-induced oxidation of biogenic volatile organic compounds and ambient lifetimes, Atmos. Chem. Phys., 19, 10391-10403, doi:10.5194/acp-19-10391-2019, 2019.

Lin C., Hu, R., Xie, P., Lou, S., Zhang, G., Tong, J., Liu, J., and Liu, W.: Nocturnal atmospheric chemistry of NO(3) and N(2)O(5) over Changzhou in the Yangtze River Delta in China, J Environ Sci (China), 114, 376-390,

https://doi.org/10.5194/egusphere-2026-4552
Preprint. Discussion started: 25 August 2026

doi:10.1016/j.jes.2021.09.016, 2022.

Lin C., Huang, R.-J., Duan, J., Zhong, H., and Xu, W.: Primary and Secondary Organic Nitrate in Northwest China: A Case Study, Environmental Science & Technology Letters, 8, 947-953, doi:10.1021/acs.estlett.1c00692, 2021.

Lin P., Bluvshtein, N., Rudich, Y., Nizkorodov, S. A., Laskin, J., and Laskin, A.: Molecular chemistry of atmospheric brown carbon inferred from a nationwide biomass burning event, Environmental science technology, 51, 11561-11570, 2017.

Ling Z. H., Guo, H., Cheng, H. R., and Yu, Y. F.: Sources of ambient volatile organic compounds and their contributions to photochemical ozone formation at a site in the Pearl River Delta, southern China, Environ Pollut, 159, 2310-2319, doi:10.1016/j.envpol.2011.05.001, 2011.

Liu T., Wang, Z., Huang, D. D., Wang, X., and Chan, C. K.: Significant Production of Secondary Organic Aerosol from Emissions of Heated Cooking Oils, Environmental Science & Technology Letters, 5, 32-37, doi:10.1021/acs.estlett.7b00530, 2017.

Liu Y., Shen, H., Mu, J., Li, H., Chen, T., Yang, J., Jiang, Y., Zhu, Y., Meng, H., Dong, C., Wang, W., and Xue, L.: Formation of peroxyacetyl nitrate (PAN) and its impact on ozone production in the coastal atmosphere of Qingdao, North China, Sci Total Environ, 778, 146265, doi:https://doi.org/10.1016/j.scitotenv.2021.146265, 2021.

Liu Y., Wu, L., Huang, S., Song, Q., Hu, W., Chen, W., Wu, Z., Man, R., He, Y., Li, W., Peng, Y., Liu, J., Song, W., Ma, N., Yuan, B., Wang, X., and Shao, M.: Sources, size-resolved deposition in the human respiratory tract and health risks of submicron black carbon in urban atmosphere in Pearl River Delta, China, Sci Total Environ, 891, 164391, doi:https://doi.org/10.1016/j.scitotenv.2023.164391, 2023.

Mao J., Paulot, F., Jacob, D. J., Cohen, R. C., Crounse, J. D., Wennberg, P. O., Keller, C. A., Hudman, R. C., Barkley, M. P., and Horowitz, L. W.: Ozone and organic nitrates over the eastern United States: Sensitivity to isoprene chemistry, Journal of Geophysical Research: Atmospheres, 118, 11,256-211,268, doi:10.1002/jgrd.50817, 2013.

McLafferty F. W., and Turecek, F.: Interpretation of mass spectra. Fourth edition, 371 pp., University Science Books, doi:https://doi.org/10.1002/bms.1200230614,1993.

Middlebrook A. M., Bahreini, R., Jimenez, J. L., and Canagaratna, M. R.: Evaluation of composition-dependent collection efficiencies for the aerodyne aerosol mass spectrometer using field data, Aerosol Science and Technology, 46, 258-271, 2012.

Nah T., Sanchez, J., Boyd, C. M., and Ng, N. L.: Photochemical Aging of alpha-pinene and beta-pinene Secondary Organic Aerosol formed from Nitrate Radical Oxidation, Environ Sci Technol, 50, 222-231, doi:10.1021/acs.est.5b04594, 2016.

Ng N. L., Brown, S. S., Archibald, A. T., Atlas, E., Cohen, R. C., Crowley, J. N., Day, D. A., Donahue, N. M., Fry, J. L., Fuchs, H., Griffin, R. J., Guzman, M. I., Herrmann, H., Hodzic, A., Iinuma, Y., Jimenez, J. L., Kiendler-Scharr, A., Lee, B. H., Luecken, D. J., Mao, J., McLaren, R., Mutzel, A., Osthoff, H. D., Ouyang, B., Picquet-Varrault, B., Platt, U., Pye, H. O. T., Rudich, Y., Schwantes, R. H., Shiraiwa, M., Stutz, J., Thornton, J. A., Tilgner, A., Williams, B. J., and Zaveri, R. A.: Nitrate radicals and biogenic volatile organic compounds: oxidation, mechanisms, and organic aerosol, Atmos. Chem. Phys., 17, 2103-2162, doi:10.5194/acp-17-2103-2017, 2017.

Ning X., Wang, Y., Zhu, N., Li, G., and Sang, N.: Risk assessment of the lipid metabolism-disrupting effects of nitro-PAHs, J

https://doi.org/10.5194/egusphere-2026-4552
Preprint. Discussion started: 25 August 2026

Hazard Mater, 396, 122611, doi:10.1016/j.jhazmat.2020.122611, 2020.

Onasch T., Trimborn, A., Fortner, E., Jayne, J., Kok, G., Williams, L., Davidovits, P., and Worsnop, D.: Soot particle aerosol mass spectrometer: development, validation, and initial application, Aerosol Science and Technology, 46, 804-817, 2012.

Peng W., McCaffery, C., Kuittinen, N., Rönkkö, T., Cocker, D. R., and Karavalakis, G.: Secondary Organic and Inorganic Aerosol Formation from a GDI Vehicle under Different Driving Conditions, Atmosphere, 13, doi:10.3390/atmos13030433, 2022.

Perring A. E., Pusede, S. E., and Cohen, R. C.: An observational perspective on the atmospheric impacts of alkyl and multifunctional nitrates on ozone and secondary organic aerosol, Chem Rev, 113, 5848-5870, doi:10.1021/cr300520x, 2013.

Pullinen I., Schmitt, S., Kang, S., Sarrafzadeh, M., Schlag, P., Andres, S., Kleist, E., Mentel, T. F., Rohrer, F., Springer, M., Tillmann, R., Wildt, J., Wu, C., Zhao, D., Wahner, A., and Kiendler-Scharr, A.: Impact of NOx on secondary organic aerosol (SOA) formation from α-pinene and β-pinene photooxidation: the role of highly oxygenated organic nitrates, Atmos. Chem. Phys., 20, 10125-10147, doi:10.5194/acp-20-10125-2020, 2020.

Qiu C., and Zhang, R.: Multiphase chemistry of atmospheric amines, Phys Chem Chem Phys, 15, 5738-5752, doi:10.1039/c3cp43446j, 2013.

Ramasamy S., Nakayama, T., Imamura, T., Morino, Y., Kajii, Y., and Sato, K.: Investigation of dark condition nitrate radical- and ozone-initiated aging of toluene secondary organic aerosol: Importance of nitrate radical reactions with phenolic products, Atmospheric Environment, 219, 117049, 2019.

Ren J., Guo, F., and Xie, S.: Diagnosing ozone–NOx–VOC sensitivity and revealing causes of ozone increases in China based on 2013–2021 satellite retrievals, Atmos. Chem. Phys., 22, 15035-15047, doi:10.5194/acp-22-15035-2022, 2022.

Ren Y., Wu, Z., Bi, F., Li, H., Zhang, H., Li, J., Gao, R., Long, F., Liu, Z., Ji, Y., and Wang, G.: Significant contributions of biomass burning to PM2.5-bound aromatic compounds: insights from field observations and quantum chemical calculations, Atmos. Chem. Phys., 25, 6975-6990, doi:10.5194/acp-25-6975-2025, 2025.

Rollins A., Pusede, S., Wooldridge, P., Min, K. E., Gentner, D., Goldstein, A., Liu, S., Day, D., Russell, L., and Rubitschun, C.: Gas/particle partitioning of total alkyl nitrates observed with TD-LIF in Bakersfield, Journal of Geophysical Research: Atmospheres, 118, 6651-6662, 2013.

Rollins A. W., Browne, E. C., Min, K. E., Pusede, S. E., Wooldridge, P. J., Gentner, D. R., Goldstein, A. H., Liu, S., Day, D. A., Russell, L. M., and Cohen, R. C.: Evidence for NO(x) control over nighttime SOA formation, Science, 337, 1210-1212, doi:10.1126/science.1221520, 2012.

Sato K., Ikemori, F., Ramasamy, S., Iijima, A., Kumagai, K., Fushimi, A., Fujitani, Y., Chatani, S., Tanabe, K., Takami, A., Tago, H., Saito, Y., Saito, S., Hoshi, J., and Morino, Y.: Formation of secondary organic aerosol tracers from anthropogenic and biogenic volatile organic compounds under varied NOx and oxidant conditions, Atmospheric Environment: X, 14, 100169, doi:https://doi.org/10.1016/j.aeaoa.2022.100169, 2022.

Sun J., Li, Z., Xue, L., Wang, T., Wang, X., Gao, J., Nie, W., Simpson, I. J., Gao, R., Blake, D. R., Chai, F., and Wang, W.:

https://doi.org/10.5194/egusphere-2026-4552
Preprint. Discussion started: 25 August 2026

Summertime C1-C5 alkyl nitrates over Beijing, northern China: Spatial distribution, regional transport, and formation mechanisms, Atmospheric Research, 204, 102-109, doi:10.1016/j.atmosres.2018.01.014, 2018.

Sun Y. L., Zhang, Q., Schwab, J. J., Demerjian, K. L., Chen, W. N., Bae, M. S., Hung, H. M., Hogrefe, O., Frank, B., Rattigan, O. V., and Lin, Y. C.: Characterization of the sources and processes of organic and inorganic aerosols in New York city with a high-resolution time-of-flight aerosol mass apectrometer, Atmospheric Chemistry and Physics, 11, 1581-1602, doi:10.5194/acp-11-1581-2011, 2011.

Walters W. W., Takeuchi, M., Blum, D. E., Eris, G., Tanner, D., Xu, W., Rivera-Rios, J., Liu, F., Xu, T., Huey, G., Min, J. B., Weber, R., Ng, N. L., and Hastings, M. G.: Evaluating NOx fate and organic nitrate chemistry from α-pinene oxidation using stable oxygen and nitrogen isotopes, Atmos. Chem. Phys., 25, 10707-10730, doi:10.5194/acp-25-10707-2025, 2025.

Wang H., Chen, X., Lu, K., Hu, R., Li, Z., Wang, H., Ma, X., Yang, X., Chen, S., Dong, H., Liu, Y., Fang, X., Zeng, L., Hu, M., and Zhang, Y.: NO3 and N2O5 chemistry at a suburban site during the EXPLORE-YRD campaign in 2018, Atmospheric Environment, 224, doi:10.1016/j.atmosenv.2019.117180, 2020.

Wu C., Wu, D., and Yu, J. Z.: Quantifying black carbon light absorption enhancement with a novel statistical approach, Atmos. Chem. Phys., 18, 289-309, doi:10.5194/acp-18-289-2018, 2018.

Wu L., Huang, S., Liu, Y., Song, Q., Hu, W., Chen, W., Kuang, Y., Wang, X., Li, W., Peng, Y., Chen, D., Yue, D., Song, W., Yuan, B., Wang, X., and Shao, M.: Source, formation mechanism and inhalation deposition flux of organic aerosols in urban and rural areas of the Pearl River Delta, Acta Scientiae Circumstantiae (China), 44, 15-28, doi:10.13671/j.hjkxxb.2023.0194, 2024a.

Wu Y., Liu, Q., Liu, D., Tian, P., Xu, W., Wang, J., Hu, K., Li, S., Jiang, X., Wang, F., Huang, M., Ding, D., Yu, C., and Hu, D.: Enhanced formation of nitrogenous organic aerosols and brown carbon after aging in the planetary boundary layer, npj Climate and Atmospheric Science, 7, 179, doi:10.1038/s41612-024-00726-x, 2024b.

Xu L., Guo, H., Boyd, C. M., Klein, M., Bougiatioti, A., Cerully, K. M., Hite, J. R., Isaacman-VanWertz, G., Kreisberg, N. M., Knote, C., Olson, K., Koss, A., Goldstein, A. H., Hering, S. V., de Gouw, J., Baumann, K., Lee, S. H., Nenes, A., Weber, R. J., and Ng, N. L.: Effects of anthropogenic emissions on aerosol formation from isoprene and monoterpenes in the southeastern United States, Proc Natl Acad Sci U S A, 112, 37-42, doi:10.1073/pnas.1417609112, 2015a.

Xu L., Suresh, S., Guo, H., Weber, R. J., and Ng, N. L.: Aerosol characterization over the southeastern United States using high-resolution aerosol mass spectrometry: spatial and seasonal variation of aerosol composition and sources with a focus on organic nitrates, Atmospheric Chemistry and Physics, 15, 7307-7336, doi:10.5194/acp-15-7307-2015, 2015b.

Xu W., Sun, Y., Wang, Q., Du, W., Zhao, J., Ge, X., Han, T., Zhang, Y., Zhou, W., Li, J., Fu, P., Wang, Z., and Worsnop, D. R.: Seasonal Characterization of Organic Nitrogen in Atmospheric Aerosols Using High Resolution Aerosol Mass Spectrometry in Beijing, China, ACS Earth and Space Chemistry, 1, 673-682, doi:10.1021/acsearthspacechem.7b00106, 2017.

Xu W., Takeuchi, M., Chen, C., Qiu, Y., Xie, C., Xu, W., Ma, N., Worsnop, D. R., Ng, N. L., and Sun, Y.: Estimation of particulate organic nitrates from thermodenuder–aerosol mass spectrometer measurements in the North China Plain,

https://doi.org/10.5194/egusphere-2026-4552
Preprint. Discussion started: 25 August 2026

Atmospheric Measurement Techniques, 14, 3693-3705, doi:10.5194/amt-14-3693-2021, 2021a.

Xu Z. N., Nie, W., Liu, Y. L., Sun, P., Huang, D. D., Yan, C., Krechmer, J., Ye, P. L., Xu, Z., Qi, X. M., Zhu, C. J., Li, Y. Y., Wang, T. Y., Wang, L., Huang, X., Tang, R. Z., Guo, S., Xiu, G. L., Fu, Q. Y., Worsnop, D., Chi, X. G., and Ding, A. J.: Multifunctional Products of Isoprene Oxidation in Polluted Atmosphere and Their Contribution to SOA, Geophysical Research Letters, 48, doi:10.1029/2020gl089276, 2021b.

Yang S., Yuan, B., Peng, Y., Huang, S., Chen, W., Hu, W., Pei, C., Zhou, J., Parrish, D. D., Wang, W., He, X., Cheng, C., Li, X. B., Yang, X., Song, Y., Wang, H., Qi, J., Wang, B., Wang, C., Wang, C., Wang, Z., Li, T., Zheng, E., Wang, S., Wu, C., Cai, M., Ye, C., Song, W., Cheng, P., Chen, D., Wang, X., Zhang, Z., Wang, X., Zheng, J., and Shao, M.: The formation and mitigation of nitrate pollution: comparison between urban and suburban environments, Atmos. Chem. Phys., 22, 4539-4556, doi:10.5194/acp-22-4539-2022, 2022.

Yang X. Y., Igarashi, K., Tang, N., Lin, J. M., Wang, W., Kameda, T., Toriba, A., and Hayakawa, K.: Indirect- and direct-acting mutagenicity of diesel, coal and wood burning-derived particulates and contribution of polycyclic aromatic hydrocarbons and nitropolycyclic aromatic hydrocarbons, Mutat Res, 695, 29-34, doi:10.1016/j.mrgentox.2009.10.010, 2010.

Ye C., Yuan, B., Lin, Y., Wang, Z., Hu, W., Li, T., Chen, W., Wu, C., Wang, C., Huang, S., Qi, J., Wang, B., Wang, C., Song, W., Wang, X., Zheng, E., Krechmer, J. E., Ye, P., Zhang, Z., Wang, X., Worsnop, D. R., and Shao, M.: Chemical characterization of oxygenated organic compounds in the gas phase and particle phase using iodide CIMS with FIGAERO in urban air, Atmospheric Chemistry and Physics, 21, 8455-8478, doi:10.5194/acp-21-8455-2021, 2021.

Yu D., Tan, Z., Lu, K., Ma, X., Li, X., Chen, S., Zhu, B., Lin, L., Li, Y., Qiu, P., Yang, X., Liu, Y., Wang, H., He, L., Huang, X., and Zhang, Y.: An explicit study of local ozone budget and NOx-VOCs sensitivity in Shenzhen China, Atmospheric Environment, 224, doi:10.1016/j.atmosenv.2020.117304, 2020.

Yu K., Zhu, Q., Du, K., and Huang, X.-F.: Characterization of nighttime formation of particulate organic nitrates based on high-resolution aerosol mass spectrometry in an urban atmosphere in China, Atmos. Chem. Phys., 19, 5235-5249, doi:10.5194/acp-19-5235-2019, 2019.

Yu X., Li, Q., Liao, K., Li, Y., Wang, X., Zhou, Y., Liang, Y., and Yu, J. Z.: New measurements reveal a large contribution of nitrogenous molecules to ambient organic aerosol, npj Climate and Atmospheric Science, 7, 72, doi:10.1038/s41612-024-00620-6, 2024.

Yuan B., Liu, Y., Shao, M., Lu, S., and Streets, D. G.: Characterization of typical biomass burning tracers among atmospheric particles in urban Guangzhou, Environ Sci Technol, 44, 4577-4582, 2010.

Zahardis J G. S., Petrucci G A: The ozonolysis of primary aliphatic amines in fine particles, Atmospheric Chemistry and Physics, 8, 1181-1194, 2008.

Zeng L., Fan, G.-J., Lyu, X., Guo, H., Wang, J.-L., and Yao, D.: Atmospheric fate of peroxyacetyl nitrate in suburban Hong Kong and its impact on local ozone pollution, Environmental Pollution, 252, 1910-1919, doi:https://doi.org/10.1016/j.envpol.2019.06.004, 2019.

Zhang C., Ji ,: Characterization of submicron particles during biomass burning and coal combustion periods in Beijing, China,

https://doi.org/10.5194/egusphere-2026-4552
Preprint. Discussion started: 25 August 2026

Science of the Total Environment, 562, 812-821, doi:10.1016/j.scitotenv.2016.04.015, 2016.

Zhang J. K., Sun, Y., Liu, Z. R., Ji, D. S., Hu, B., Liu, Q., and Wang, Y. S.: Characterization of submicron aerosols during a serious pollution month in Beijing (2013) using an aerodyne high-resolution aerosol mass spectrometer, Atmospheric Chemistry & Physics Discussions, 13, doi:10.5194/acpd-13-19009-2013, 2013.

Zhang Y., Sun, J., Zheng, P., Chen, T., Liu, Y., Han, G., Simpson, I. J., Wang, X., Blake, D. R., Li, Z., Yang, X., Qi, Y., Wang, Q., Wang, W., and Xue, L.: Observations of C(1)-C(5) alkyl nitrates in the Yellow River Delta, northern China: Effects of biomass burning and oil field emissions, Sci Total Environ, 656, 129-139, doi:10.1016/j.scitotenv.2018.11.208, 2019.

Zhou S., Collier, S., Jaffe, D. A., and Zhang, Q.: Free tropospheric aerosols at the Mt. Bachelor Observatory: more oxidized and higher sulfate content compared to boundary layer aerosols, Atmospheric Chemistry and Physics, 19, 1571-1585, doi:10.5194/acp-19-1571-2019, 2019.

Zhu Q., Cao, L.-M., Tang, M.-X., Huang, X.-F., Saikawa, E., and He, L.-Y.: Characterization of organic aerosol at a rural site in the North China Plain region: Sources, volatility and organonitrates, Advances in Atmospheric Sciences, 38, 1115-1127, 2021.

Zhu Q., He, L.-Y., Huang, X.-F., Cao, L.-M., Gong, Z.-H., Wang, C., Zhuang, X., and Hu, M.: Atmospheric aerosol compositions and sources at two national background
sites in northern and southern China, Atmospheric Chemistry and Physics, 16, 10283-10297, doi:10.5194/acp-16-10283-2016, 2016.

Zhu W., Shi, J., Guo, S., Wang, Q., Chen, J., Lou, S., and Hu, M.: Comparative analysis of methods for seasonal particulate organic nitrate estimation in urban areas, npj Climate and Atmospheric Science, 8, 21, doi:10.1038/s41612-025-00904-5, 2025.